sustainability

IMPACT FACTOR 3.3

CITESCORE 7.7

Article

# Contamination Analysis of an Old Croatian Industrial Site and Proposals for Its Planned Remediation and Repurposing

Želimir Veinović, Dario Perković and Ivica Prlić

Special Issue
Land Use and Sustainable Environment Management

Edited by
Dr. Heera Lee, Dr. Bora Lee and Dr. Byoung Ki Choi

MDPI

https://doi.org/10.3390/su18083897

*sustainability*

MDPI

*Article*

# Contamination Analysis of an Old Croatian Industrial Site and Proposals for Its Planned Remediation and Repurposing

**Želimir Veinović [1], Dario Perković [1,*] and Ivica Prlić [2]**

[1] Faculty of Mining, Geology and Petroleum Engineering, University of Zagreb, Pierottijeva 6, HR 10000 Zagreb, Croatia; zelimir.veinovic@rgn.unizg.hr
[2] Institute for Medical Research and Occupational Health, Ksaverska Cesta 2, HR 10001 Zagreb, Croatia; iprlic@imi.hr
* Correspondence: dario.perkovic@rgn.unizg.hr

**Abstract**

The location of the decommissioned factory of plastics and chemical products Jugovinil, City of Kaštela, Croatia, has gained significant attention for urban development and the establishment of tourist facilities over the past three decades. Since the site is on the coast of the Adriatic Sea, on the shore of Kaštela Bay, where nautical tourism is already developed, plans for a five-star tourism complex were initiated. Given that the former industrial plant, its coal-powered power plant, and other later industrial activities (small shipyards) caused a certain degree of contamination with NORM (naturally occurring radioactive material) residues and heavy metals, an on-site detailed investigation was conducted into the spatial distribution and concentration evaluation of contaminants within dozens of soil samples, and the distributions of contaminants in the area of interest were shown in the form of maps. This study applies an integrated GIS and geostatistical framework to analyze the spatial distribution of multiple contaminants. Maps highlighting polluted zones are included, along with maps indicating areas with higher cumulative concentrations of contaminants. This paper provides an overview of potential issues related to the detected contaminants, as well as proposals for remediation methods before repurposing the site using retrospective data about sources of residues and contaminants.

**Keywords:** industrial site; remediation; urbanization; contamination; NORM residues; heavy metals; Republic of Croatia



Academic Editors: Heera Lee, Bora Lee and Byoung Ki Choi

Received: 13 March 2026
Revised: 3 April 2026
Accepted: 9 April 2026
Published: 15 April 2026



## 1. Introduction

Ex-industrial and other brownfield sites are sometimes "lost forever" since anthropogenic activities occasionally cause irreparable effects or ones that are too costly to remediate. In cases of large amounts of waste mineral material deposited in certain locations, several issues can emerge:

- The quantities are too large to remove from the site;
- There are no potential secondary disposal locations at distances that would justify the costs of moving materials;
- The properties of materials do not allow removal from the site or simple and economically acceptable remediation in situ, such as applying greening, urbanization or other types of sustainable remediation.

Reversing the state of sites affected with legacy waste from old, unsustainable industries often means dealing with locations covered with overwhelming amounts of materials,

sometimes containing heavy metals, NORM residues and other hazardous materials which are contaminating certain locations.

Losing space at brownfield sites means exhausting a resource, which has environmental, societal and economic consequences on resource needs that are "compromising the ability of future generations to meet theirs". Hence, dealing with such old industrial sites with the purpose of remediation and reclamation of the location represents a sustainable practice in both environmental and economic terms. Remediation of brownfield sites containing mineral waste can reverse the state of ecosystems affected by deposited material and remove or mitigate risk to biota caused by contaminants. Such sites are an opportunity to apply sustainability initiatives, such as freeing up space for new industry, urbanization or even revegetation and other types of ecological enhancement. In an economic sense, "lost industrial sites", such as the one in Kaštela Bay, Croatia, can provide space for responsible economic growth.

The aim of the research presented in this paper, similar to much other research of the same type [1–9], is the reclamation and repurposing of an ex-industrial site, that is, the former "factory of plastics and chemical products, Jugovinil", City of Kaštela, Croatia, located on the coastline of the Croatian part of the Adriatic Sea on the shore of Kaštela Bay (Figure 1).

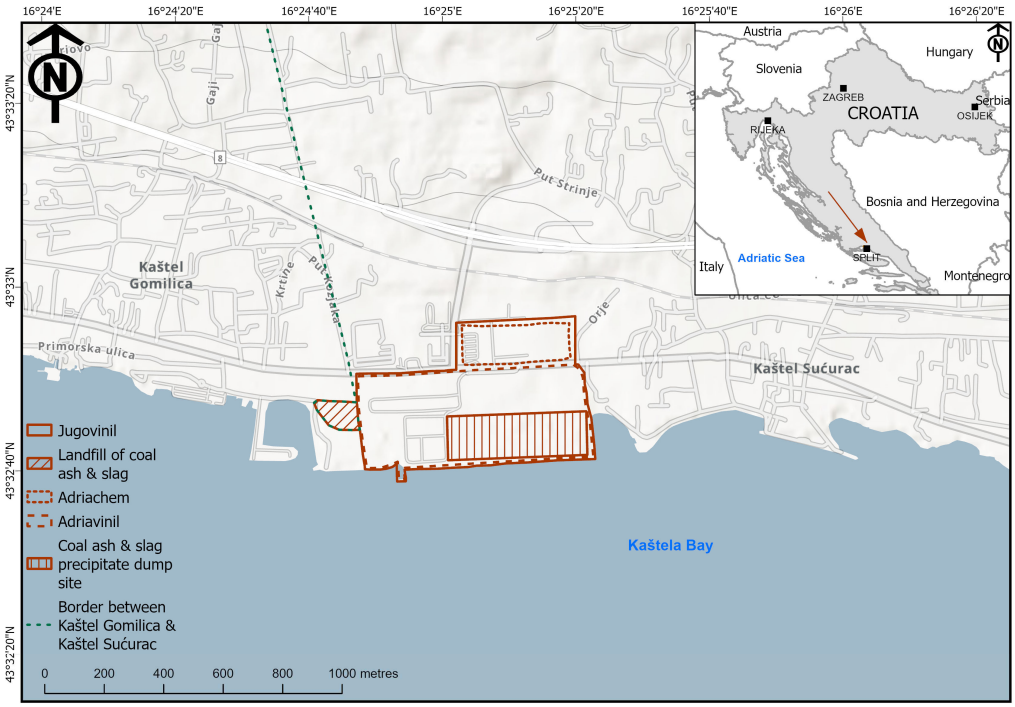


**Figure 1.** Location of the former factory of plastics and chemical products "Jugovinil" within the City of Kaštela.

Tourism in Croatia contributes approximately 20% of its GDP [10], with a total of 21.8 million tourists visiting in 2025 [11], which clearly signifies that it is of national interest to remediate old, decommissioned industrial sites on the coast, as well as other brownfield sites, and convert them into tourist centers or some other economically useful site (e.g., small photovoltaic power stations—solar parks), or redevelop them in a way that they remain in harmony with the environment (greening projects supporting the current policies related to climate changes).

There is a noteworthy number of ex-industrial and other brownfield sites in Croatia that already have undergone or are planned to undergo remediation and repurposing, and some of them are significantly polluted with heavy metals or other contaminants [12].

While several of them have been remediated and repurposed, some are still waiting for on-site screening and research to determine the state of contamination, design remediation project documentation, licensing, or financial means for implementation. However, the case of the former Jugovinil factory is specific and interesting for several reasons:

- It is located on the very coast of the Adriatic Sea, on Kaštela Bay, within an important tourist center of the City of Kaštela (see Figure 1), and surrounded by other important tourist centers: Trogir, Solin (suburb of Split), the City of Split and Čiovo Island.
- On the site is a so-called "old repository of coal ash and slag from other coal-powered thermal power plants in the former Socialist Federative Republic of Yugoslavia (SFRY)", a landfill of NORM residues built in 1973 and fully regulated.
- The site contains a coal ash and slag tailings repository from the power plant of the former Jugovinil factory, which are identified as NORM (naturally occurring radioactive material) residues.
- Jugovinil was split into two industrial entities, ADRIACHEM d.d. and ADRIAVINIL d.d. (both state-owned companies), during the 1990s after the Republic of Croatia became independent, and at the beginning of the 2000s, the companies were privatized. ADRIAVINIL d.d. has not functioned as a chemical factory since 2004, and the location has become a site with small shipyards and storage facilities. Over the next 15 years, most of the industrial objects were dismantled and the parcel containing coal ash and slag tailings was regulatorily declared as a future "maritime area" owned by the Republic of Croatia. This land parcel is regarded as the county's "environmental black spot" and is to be remediated.

Figure 1 shows four significant zones: the old landfill (regulated disposal site) of coal ash and slag transferred from other coal power plants in the former SFRY, which is closed and under institutional control, the zone where ADRIACHEM d.d. was situated, and the zone where ADRIAVINIL d.d. was situated, which is the main area of interest for this paper because it contains the fourth zone—the coal and ash precipitate disposal site.

According to The Radioactive Waste, Disused Sources and Spent Nuclear Fuel Management Strategy [13] and Decision on National program for implementation of strategy of radioactive waste, disused sources and spent nuclear fuel management (Program till 2025 with glance till 2060) [14], Croatia has three officially recognized locations with NORM residues:

- Coal ash and slag disposal sites of the coal-fired power plants Plomin I and II (underwent reclamation and are under constant institutional control).
- Phosphogypsum disposal site of Petrokemija d. d., Fertilizer Factory, Kutina (soon to undergo a reclamation utilizing reuse technology in the construction industry: phosphogypsum is in the process of reevaluation as a by-product that may be used for construction and agriculture purposes [15–19] and not treated as a waste or NORM residue).
- Coal ash and slag solid precipitate dump site in Kaštela Bay from the power plant of the ex-Jugovinil factory in Kaštela Bay, which is still not fully regulated, remediated, or under proper regulatory oversight.

However, there are many smaller locations in Croatia that are not included in the previous list of officially recognized NORM residue sites and are also not properly regulated [20]:

- Temporary dumpsites for waste (mineral) materials (NORM residues) from oil and gas production;
- Dumpsites for slag and waste from primary iron production;
- Dumpsites for calcific scale and similar materials from underground water filtration plants;

- Other locations where natural radionuclides from various geological materials are industrially concentrated.

Considering the second list, the locations mentioned are not considered as a significant problem due to smaller amounts of contaminants and NORM residues with low activity, except maybe those related to oil and gas production. The official regulatory decision on whether those locations are to be researched in detail, which would help make an official decision on how to deal with those locations and the materials they contain, is still outstanding.

The ash and slag precipitate dump site of the decommissioned power plant in Kaštela Bay was taken into consideration because of the plan to reclaim this location to be urbanized and adjusted for tourist or small green production facility purposes. Detailed research was done on the whole area of the former Jugovinil industrial site [21–24] to assess the condition of the site, identify contaminants, determine its impact on the environment and potential impact on biota, perform risk assessment followed by remediation protocols and, in the case of repurposing the location, build up the regulatory matrix of construction activities.

The site of interest for this paper is situated partly in Kaštel Sućurac and partly in the neighboring Kaštel Gomilica (municipalities belonging to the City of Kaštela, Figure 1), and it can be divided into several areas of research interest (Figure 2).

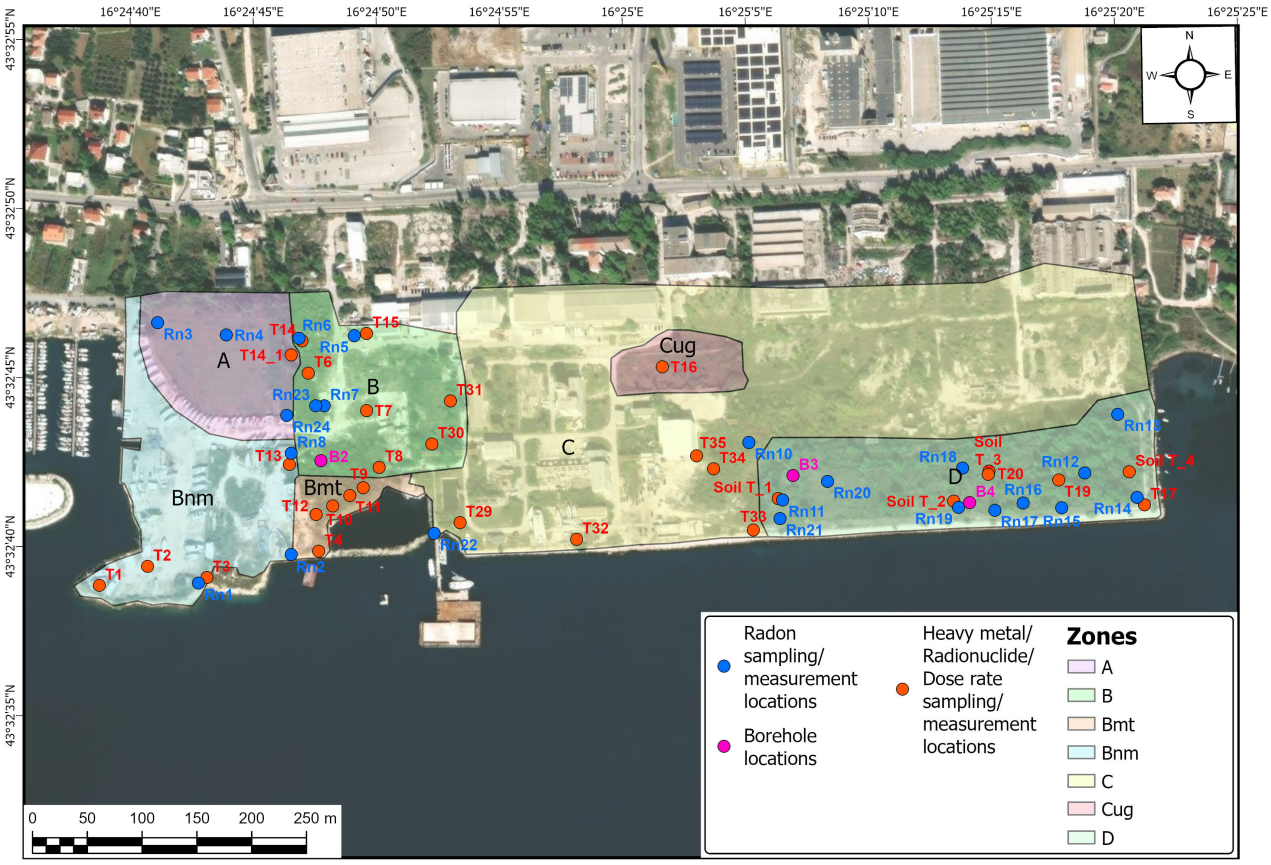


**Figure 2.** Zones of radiological and heavy metal research interest at the location of the City of Kaštela related to the former Jugovinil factory and recent small industrial activities.

As shown in Figure 2, the site is divided according to type of contaminant and history of contamination as follows:

- Zone "A"—NORM residue disposal site in Kaštel Gomilica, under regulatory oversight, containing 38,000 $m^3$ of coal combustion residuals transported from different coal-fired power plants in the former SFRY. Although the material is in fact NORM

residue (coal ash and slug), according to the "Decision of the sanitary inspectorate" [25], it is defined as "uranium ore tailings from coal" due to the high percentage of uranium in certain coals extracted and utilized in the former SFRY. Materials disposed of at this regulated disposal site are "leftovers" from the SFRY's program for the extraction of uranium from U-238/U-235-rich NORM residues and experimental processing to yellow cake, which ended in 1973 [26], and the disposal site was engineered to specifications and formally decommissioned, preventing further activity in the same year. Most of the area of this zone is under a concession contract entrusted for use to a private enterprise, Marina Kaštela d.o.o., in 2014 for the duration of 30 years, under the condition of being safeguarded and not disturbed in any way. Since the disposal site is closed and under regulatory oversight, this area is not of primary interest to this paper, although part of the carried-out research encompasses it.

- Zone "B"—Originally a natural depression backfilled twice: the first time during the 1970s and 1980s, with coal ash and slag from Jugovinil's power plant and construction and demolition waste used to prepare the location for the construction of reservoirs for chemicals; the second time during the second half of 2015 to prepare the location for the operating area of the current marina.
- Zone "Bnm"—An area created during the last three decades (since the area was given into concession) by dumping waste rock and soil into the sea (excavated material from other locations: during the building of a commercial center in the city of Split, Croatia, construction of a highway nearby Split, etc.) in order to construct a marina, berth, mooring and dry dock with the supporting facilities.
- Zone "Bmt"—An area partially backfilled with coal combustion residuals mostly from Jugovinil's power plant and some construction and demolition waste, to relieve space in the precipitate disposal area (Zone "D").
- Zone "C"—A zone that originally contained coal combustion residuals but was remediated in 1971–1973, and the material was relocated to Zone "A". Zone "C" was then covered with earthwork material and a certain amount of construction waste to prepare ground for the construction of a new factory installation in 1974.
- Zone "Cug"—An area used to store coal for Jugovinil's power plant since the beginning of factory production (1947).
- Zone "D"—The coal combustion residual precipitate disposal site (in Kaštel Sućurac) composed of 180,000 $m^3$ of combustion residuals deposited from the ex-Jugovinil factory's local power plant, utilizing hydro-transport of the material, which precipitated in a specifically designed and protected zone created by the construction of the seawall and filling the consequently gained area with geological material. The outer wall of the disposal site (seawall) now forms the wave attenuator of Kaštela Bay. The disposal site was formed in the 1980s and utilized till the 2000s.
- Unmarked—Several smaller contaminated areas containing combustion residuals form the local power plant (100,000 $m^3$ in total) along the abovementioned zones, created mostly while maintaining the factory in the operational and demolition period.

Most of the abovementioned areas are unused and not frequented by people (apart from the marina). Regarding the general biota in the wider area of this ex-industrial site, the entire precipitate dump site (Zone "D") is covered with wild vegetation in an advanced stage of growth (Lugistrum vulgaris, Tamaricaceae gallica, Weissia dalmatica, Spartium junceum, Satureja subspicata, Myrto-Pistacietum lentisci, Vitici-Tamaricetum dalmaticae, etc.), and there are many examples of autochthonous fauna [21–24,27]. Detailed research on the marine biota in this area was done as well [22,24,27], but is not part of this paper.

## 2. Materials and Methods

Most of the research on the location was done during 2009–2011 [21–24], although some is more recent [27], and further research is planned for 2026. Earlier research was done thoroughly, and the most recent research is mostly intended to assess the impact of anthropogenic activities and meteorological events that occurred in the last 15 years. In addition, recent data is needed to meet regulatory requirements for the remediation of the area.

Original research included detailed mapping; determination of the basic geological, hydrogeological and seismic properties of the location; sampling of soil and rock material from the surface (composite samples from 1 $m^2$ surfaces and 15 cm in depth, which is a standard procedure used for environmental site assessment, as well as for agronomic soil testing—collecting samples from a defined surface area, "quadrat", at a specific depth that represents the most active biological layer) and seabed along the coastline in the vicinity of the location; cores from exploratory boreholes; and sampling groundwater. Regarding biota, samples of surface organisms (plants) and the sea (benthic samples) were taken, and special research was done related to endemic species found at the precipitate dump site (Zone "D") [27]. All aforementioned samples were analyzed by measuring heavy metal and radionuclide concentrations. Measurements of the ambient dose rate (H*(10)/t; trace method) were taken on the surface of the location (including local natural background activity) and on the surface of the seabed (special well drilling probe trace method), and VR gamma spectrometry was used to measure radon concentration from the soil. Similar research was done to "measure the levels of radionuclides, contributing to the sustainable management of campus environments" [28] and to establish baseline data on natural radioactivity in Mexican soils "to facilitate comparison with global reference values, and to design informed radiation protection strategies and environmental management decisions" [29].

The research presented in this paper is related to the distribution of heavy metals in soil, dose-rate measurements, activity concentrations of radionuclides measured in situ, laboratory-measured activity concentrations of radionuclides, and laboratory gamma spectrometry measurements of radon exhalation rates from samples. Other measurements and their results, such as forensic research on coals used during the period of power plant operation, determining the U238/U235 ratio, and recent in situ measurements of Rn-222 concentration in coal ash "soil gas", are planned to be presented and discussed in future publications.

To carry out the research in a proper way, it was necessary to perform a complete geodetic survey of the location, among other things, to precisely determine the waterline and the line of the coast. The data were obtained by surveying the land and measuring the sea depth (determining the depth relief of Kaštela Bay) [23]. This situational plan is the cornerstone for cartographic representations in this study, and it is supported with digital orthophoto imagery.

The underlying purpose for studying the seafloor and marine life was the engineering of a precipitator/tailings pond, where coal combustion residuals were transported by means of hydro-transport from the power plant. Water overflowed into the sea, transporting certain amounts of combustion residuals with it. To adequately explore this location, it was important to determine the types and amounts of materials transported and sedimented in the sea. While correlations between the concentrations of different heavy metals are commonly observed [30–35], as well as their correlation with the physicochemical properties of different soils [36,37], it is essential to consider the specific properties of each metal, the complexity of environmental systems, and the context of the study area when interpreting these relationships. Additionally, statistical analyses such as correlation coefficients

and multivariate techniques can help quantify and assess the strength and significance of correlations between heavy metal concentrations in environmental datasets [38–41].

The entire study area is characterized by a uniform geological setting consisting of Eocene flysch (alternating layers of sandstone and marl) deposits, with limestone as bedrock. The combination of *Terra Rossa* and weathered coal combustion residuals, as well as the chronosequence of humus formation, covers part of the area. Some locations are blanketed by construction/demolition waste and concrete dust due to the demolition of Jugovinil facilities. Samples were collected according to the IAEA sampling protocol [24,42], which considered locations (marked on Figure 2) demonstrating the key features of the location and its surroundings: dumpsites, shipyards, any other industrial activity, etc.

The Institute for Medical Research and Occupational Health (IMROH), Zagreb, Croatia, completed the following laboratory and field research: heavy metal concentrations, measurements of dose rates, in situ gamma spectrometry measurements of radionuclide activity concentrations, laboratory gamma spectrometry measurements of activity concentrations and laboratory gamma spectrometry measurements of radon exhalation rates.

## 3. Results

### *3.1. Heavy Metals*

From a representative set of 30 samples of soil (defined by balancing known properties of location, desired statistical precision and logistical constraints, e.g., approachability, availability of materials, etc.) acquired on site (Table 1), concentrations of 10 heavy metals were determined at IMROH laboratories, Zagreb, Croatia.

**Table 1.** Heavy metal concentrations in 30 coal ash samples (μg/g).

| Sample Label | Cd | Ni | Co | Cr | Tl | Pb | Mn | Cu | Zn | Fe |
|---|---|---|---|---|---|---|---|---|---|---|
| T1 | 3.63 [1] | 30.02 | 14.86 | 19.95 | 30.32 | 24.10 | 279.43 | 14.38 | 20.64 | 4159.01 |
| T2 | 4.00 | 124.09 | 23.13 | 73.68 | 26.54 | 307.38 | 634.53 | 1270.05 | 613.77 | 15,863.25 |
| T3 | 3.75 | 71.85 | 21.31 | 64.45 | 24.59 | 33.87 | 700.27 | 35.52 | 63.57 | 19,121.83 |
| T4 | 2.37 | 368.18 | 119.41 | 190.89 | 11.19 | 946.08 | 1899.59 | 2419.78 | 7394.02 | 30,096.27 |
| T6 | 5.10 | 99.19 | 20.82 | 171.68 | 21.49 | 44.24 | 366.37 | 52.25 | 120.22 | 25,864.60 |
| T7 | 4.29 | 46.02 | 14.52 | 69.17 | 20.84 | 295.20 | 285.02 | 29.89 | 701.83 | 15,847.46 |
| T8 | 4.83 | 64.20 | 18.45 | 68.05 | 24.85 | 270.79 | 376.07 | 37.06 | 420.57 | 14,684.76 |
| T9 | 5.21 | 111.29 | 20.30 | 96.10 | 22.26 | 49.79 | 291.54 | 69.52 | 190.62 | 28,649.34 |
| T10 | 6.10 | 79.86 | 19.40 | 69.93 | 25.55 | 69.05 | 252.64 | 61.04 | 333.95 | 27,453.54 |
| T11 | 5.29 | 103.29 | 21.51 | 95.31 | 22.44 | 56.85 | 343.09 | 72.92 | 196.94 | 30,473.50 |
| T12 | 5.83 | 180.34 | 70.73 | 95.32 | 25.04 | 613.86 | 924.74 | 1766.61 | 4147.97 | 36,568.74 |
| T13 | 3.76 | 37.05 | 9.19 | 49.72 | 13.57 | 26.96 | 142.38 | 43.67 | 135.65 | 8996.64 |
| T14 | 6.30 | 100.63 | 20.60 | 156.31 | 24.18 | 41.55 | 361.54 | 67.54 | 110.68 | 27,158.04 |
| T14_1 | 4.30 | 94.09 | 21.26 | 150.38 | 19.67 | 85.05 | 655.52 | 48.14 | 96.40 | 32,577.50 |
| T15 | 7.36 | 67.50 | 24.28 | 64.35 | 21.85 | 50.49 | 914.81 | 39.68 | 134.70 | 22,313.01 |
| T16 | 3.86 | 63.91 | 6.69 | 37.46 | 10.85 | 28.14 | 45.58 | 26.31 | 66.39 | 18,946.04 |
| T17 | 6.65 | 52.70 | 15.43 | 56.41 | 23.71 | 56.05 | 441.71 | 24.57 | 101.03 | 18,455.18 |
| T19 | 3.90 | 120.01 | 20.74 | 95.78 | 23.14 | 45.77 | 336.84 | 69.60 | 137.49 | 26,775.34 |
| T20 | 2.97 | 113.44 | 22.67 | 62.27 | 19.27 | 31.66 | 390.24 | 61.21 | 89.91 | 31,802.97 |
| T29 | 3.78 | 59.99 | 17.20 | 66.57 | 27.87 | 57.64 | 416.07 | 56.77 | 262.40 | 16,862.21 |
| T30 | 3.09 | 71.33 | 19.67 | 67.11 | 24.82 | 37.80 | 676.20 | 48.20 | 108.15 | 18,071.54 |
| T31 | 3.94 | 63.99 | 17.55 | 65.40 | 27.47 | 62.10 | 528.09 | 35.11 | 167.76 | 16,061.62 |
| T32 | 1.43 | 395.11 | 116.48 | 193.62 | 9.48 | 2496.64 | 2246.98 | 2450.79 | 9268.15 | 65,676.97 |
| T33 | 5.57 | 83.90 | 19.53 | 110.13 | 22.72 | 71.94 | 434.35 | 37.38 | 142.26 | 20,933.32 |
| T34 | 4.23 | 73.09 | 18.69 | 72.19 | 25.46 | 55.34 | 479.30 | 45.29 | 102.42 | 17,635.60 |
| T35 | 4.51 | 55.01 | 17.28 | 74.57 | 25.75 | 194.00 | 376.74 | 58.24 | 192.83 | 28,143.68 |
| Soil T_1 | 5.16 | 87.21 | 17.80 | 61.88 | 21.12 | 31.96 | 227.25 | 41.00 | 76.70 | 32,217.87 |
| Soil T_2 | 6.67 | 100.13 | 19.56 | 83.34 | 19.51 | 36.18 | 271.95 | 44.21 | 102.33 | 30,473.89 |
| Soil T_3 | 5.89 | 57.78 | 16.88 | 54.78 | 21.84 | 37.90 | 350.59 | 23.70 | 71.25 | 22,527.69 |
| Soil T_4 | 7.29 | 89.70 | 20.89 | 130.59 | 22.90 | 57.39 | 370.68 | 58.99 | 230.58 | 24,220.99 |

[1] All values are given in (μg/g).

### *3.2. Dose Rates*

Measurements of dose rates were the first step in radionuclide site mapping since dose rates indicate where further research is needed. The location was covered using the "trace" measurement method at 1 m height above ground level and georeferenced by satellite GPS positioning. The method used was IMI-M-AMB-01 [43], which includes x, γ, and bremsstrahlung in the environment or near the radioactive source. The method is developed with the aim of:

- Ensuring safe working conditions for workers professionally exposed to ionizing radiation;
- Assessing the expected exposure of professionally exposed workers and the general population in emergency events when the presence of a source of ionizing radiation in the environment is suspected;
- Confirming, in all other cases when it is necessary, that the test subject does not show an elevated level of radiation.

The device used for trace measurements, as well as measurements at specific given points from which the soil sampling was done, was the FH 40 G-GL Advanced Survey Meter System, Thermo Fisher Scientific, Inc., by Ansar-analitika as a representative, Zagreb, Croatia (calibrated according to ISO/IEC 17025:2017 standard [44]). Dose rates measured on location (nGy/h) at the points of interest, i.e., the sampling locations, are shown in Table 2. The measurement points (33) are marked in Figure 2, except for those that are out of the zone of interest (used as "out of the zone of interest" measurement points) and therefore not listed in Table 2.

**Table 2.** Dose rates measured on location (nGy/h) at the points of interest—sampling locations.

| Measurement Point Label | Dose Rate (nGy/h) |
|---|---|
| T1 | 40.07 |
| T2 | 36.42 |
| T3 | 41.77 |
| T4 | 34.72 |
| T5 | 502.52 |
| T6 | 557.23 |
| T7 | 326.61 |
| T8 | 213.70 |
| T9 | 475.20 |
| T10 | 306.09 |
| T11 | 383.65 |
| T12 | 316.58 |
| T13 | 210.85 |
| T14 | 550.69 |
| T15 | 119.91 |
| T16 | 291.36 |
| T17 | 141.07 |
| T18 | 79.33 |
| T19 | 557.13 |
| T20 | 607.70 |
| T21 | 535.03 |
| T22 | 597.11 |
| T23 | 459.41 |
| T24 | 286.59 |
| T25 | 278.65 |
| T26 | 303.57 |
| T29 | 91.57 |
| T30 | 126.73 |
| T31 | 115.83 |
| T32 | 72.84 |
| T33 | 160.84 |
| T34 | 190.91 |
| T35 | 78.10 |

### *3.3. In Situ Gamma Spectrometry Measurements*

Further research was undertaken by conducting in situ gamma spectrometry measurements of activity concentrations of Ra-226, Pb-214, Bi-214, Ac-228, Bi-212, Tl-208 and K-40 at 35 points at the location (Figure 2); the measured values are given in Table 3. Measurement points T27 and T28 are out of the zone of interest and therefore are not marked in Figure 2 or listed in the table. It must be noted that activity concentrations for uranium are not given since it was under the detection limit.

**Table 3.** Activity concentrations of Ra-226, Pb-214, Bi-214, Ac-228, Bi-212, Tl-208 and K-40 acquired by in situ gamma spectrometry measurements (Bq/kg).

| Measurement Point Label | Ra-226 | Pb-214 | Bi-214 | Ac-228 | Bi-212 | Tl-208 | K-40 |
|---|---|---|---|---|---|---|---|
| T1 | 19.58 ± 4.64 [2] | 33.58 ± 4.43 | 31.42 ± 6.24 | 22.81 ± 4.09 | 10.25 ± 2.64 | 27.22 ± 7.00 | 96.89 ± 7.23 |
| T2 | 19.17 ± 4.42 | 29.34 ± 4.44 | 43.19 ± 6.60 | 17.93 ± 3.87 | 6.60 ± 2.07 | 18.77 ± 6.29 | 26.20 ± 3.89 |
| T3 | 20.44 ± 4.60 | 19.90 ± 4.31 | 36.19 ± 6.19 | 28.77 ± 4.13 | 11.36 ± 2.91 | 48.19 ± 7.05 | 133.97 ± 8.53 |
| T4 | 19.35 ± 4.27 | 23.45 ± 4.08 | 27.17 ± 6.01 | 15.29 ± 3.62 | 6.60 ± 2.35 | 23.15 ± 5.24 | 93.92 ± 7.11 |
| T5 | 285.46 ± 17.13 | 587.74 ± 19.04 | 860.88 ± 29.08 | 29.66 ± 9.71 | 32.40 ± 7.21 | 38.80 ± 5.94 | 74.64 ± 8.17 |
| T6 | 295.14 ± 17.97 | 632.48 ± 19.73 | 895.81 ± 30.26 | 59.08 ± 10.31 | 29.69 ± 7.66 | 40.05 ± 6.23 | 87.00 ± 9.03 |
| T7 | 95.15 ± 12.96 | 183.45 ± 12.55 | 331.03 ± 19.54 | 25.94 ± 8.17 | 27.11 ± 6.09 | 16.90 ± 5.63 | 49.93 ± 7.08 |
| T8 | 81.89 ± 10.70 | 172.20 ± 10.91 | 111.09 ± 16.64 | 9.68 ± 6.37 | 21.47 ± 4.72 | 48.81 ± 10.89 | 61.79 ± 6.78 |
| T9 | 229.25 ± 16.20 | 544.22 ± 18.66 | 782.70 ± 28.48 | 69.65 ± 10.23 | 12.83 ± 6.94 | 102.63 ± 17.39 | 134.46 ± 9.86 |
| T10 | 87.79 ± 12.78 | 240.31 ± 13.33 | 389.35 ± 20.37 | 31.99 ± 8.32 | 12.83 ± 6.07 | 73.22 ± 13.77 | 81.57 ± 8.30 |
| T11 | 146.73 ± 14.43 | 434.40 ± 16.32 | 612.17 ± 25.25 | 33.39 ± 8.80 | 31.40 ± 6.60 | 108.89 ± 14.99 | 68.22 ± 7.97 |
| T12 | 120.63 ± 13.02 | 301.49 ± 14.31 | 460.33 ± 22.03 | 45.51 ± 8.48 | 2.57 ± 6.15 | 42.55 ± 6.77 | 115.18 ± 9.35 |
| T13 | 98.10 ± 10.32 | 223.61 ± 11.61 | 338.80 ± 18.37 | 11.39 ± 6.54 | 5.13 ± 4.41 | 26.28 ± 4.72 | 70.69 ± 6.80 |
| T14 | 276.62 ± 17.75 | 623.05 ± 19.86 | 922.43 ± 30.73 | 27.97 ± 10.19 | 35.87 ± 7.48 | 45.68 ± 6.10 | 81.57 ± 8.76 |
| T15 | 25.68 ± 7.99 | 78.14 ± 7.53 | 119.62 ± 11.33 | 48.37 ± 5.66 | 16.99 ± 3.84 | 20.65 ± 6.03 | 104.80 ± 7.72 |
| T16 | 225.88 ± 13.47 | 377.55 ± 14.80 | 530.64 ± 23.11 | 42.63 ± 7.81 | 24.03 ± 5.58 | 23.87 ± 4.93 | 69.21 ± 7.20 |
| T17 | 86.94 ± 9.19 | 162.34 ± 9.99 | 229.75 ± 15.19 | 29.82 ± 5.56 | 15.37 ± 3.79 | 14.87 ± 3.25 | 68.22 ± 6.69 |
| T18 | 28.07 ± 6.37 | 36.17 ± 5.56 | 59.57 ± 8.30 | 23.95 ± 4.48 | 10.63 ± 3.07 | 17.98 ± 4.51 | 107.77 ± 7.88 |
| T19 | 846.28 ± 17.35 | 575.20 ± 19.05 | 812.28 ± 28.82 | 49.69 ± 11.06 | 36.07 ± 7.67 | 69.46 ± 8.47 | 110.24 ± 9.87 |
| T20 | 254.09 ± 18.17 | 591.64 ± 19.72 | 909.45 ± 30.74 | 90.73 ± 11.34 | 36.95 ± 8.33 | 46.31 ± 7.84 | 139.40 ± 10.47 |
| T21 | 269.25 ± 17.43 | 590.17 ± 19.31 | 842.03 ± 29.48 | 59.96 ± 10.13 | 35.13 ± 7.66 | 48.19 ± 7.32 | 89.48 ± 8.91 |
| T22 | 257.46 ± 18.12 | 771.97 ± 21.56 | 1089.78 ± 33.15 | 40.98 ± 10.99 | 39.58 ± 8.20 | 46.93 ± 7.96 | 102.33 ± 9.02 |
| T23 | 206.10 ± 15.99 | 510.47 ± 17.86 | 740.18 ± 27.25 | 61.94 ± 9.43 | 22.36 ± 6.98 | 26.28 ± 6.41 | 111.23 ± 8.84 |
| T24 | 168.83 ± 12.62 | 454.22 ± 16.26 | 588.95 ± 24.59 | 35.81 ± 7.87 | 26.13 ± 5.61 | 18.77 ± 5.63 | 60.80 ± 6.74 |
| T25 | 167.78 ± 12.56 | 373.74 ± 14.94 | 513.16 ± 23.27 | 49.58 ± 7.88 | 23.79 ± 5.35 | 28.79 ± 5.94 | 139.90 ± 8.83 |
| T26 | 226.73 ± 13.38 | 539.20 ± 17.02 | 617.02 ± 25.39 | 64.51 ± 7.85 | 23.48 ± 5.18 | 20.65 ± 4.93 | 76.62 ± 7.30 |
| T29 | 43.16 ± 6.98 | 114.83 ± 8.09 | 144.60 ± 12.36 | 13.84 ± 4.71 | 12.08 ± 2.89 | 15.15 ± 3.86 | 76.62 ± 6.76 |
| T30 | 2.74 ± 7.81 | 45.08 ± 6.98 | 94.86 ± 11.16 | 36.20 ± 5.34 | 16.20 ± 3.88 | 22.02 ± 5.16 | 172.03 ± 9.41 |
| T31 | 55.58 ± 7.90 | 120.37 ± 8.54 | 175.07 ± 13.29 | 22.31 ± 5.00 | 18.16 ± 3.68 | 15.43 ± 4.51 | 107.27 ± 7.86 |
| T32 | 27.71 ± 6.29 | 66.72 ± 6.69 | 93.77 ± 10.31 | 13.97 ± 4.22 | 13.12 ± 3.07 | 10.64 ± 3.19 | 74.15 ± 6.41 |
| T33 | 50.52 ± 9.41 | 176.27 ± 10.37 | 253.62 ± 15.81 | 27.98 ± 6.13 | 14.66 ± 4.53 | 18.77 ± 4.68 | 86.51 ± 7.56 |
| T34 | 103.15 ± 10.38 | 217.46 ± 11.25 | 294.22 ± 17.53 | 33.70 ± 6.60 | 20.52 ± 4.94 | 18.15 ± 4.24 | 109.74 ± 8.05 |
| T35 | 10.53 ± 6.08 | 47.42 ± 6.35 | 88.46 ± 9.42 | 17.92 ± 4.06 | 10.94 ± 2.67 | 9.39 ± 3.31 | 84.53 ± 6.94 |

[2] All values are given in (Bq/kg).

### *3.4. Laboratory Gamma Spectrometry Measurements of Activity Concentrations of Radionuclides in Composite Samples*

Samples for laboratory gamma spectrometry measurements of activity concentrations (Figure 3) of K-40, U-238, Th-232 and Ra-226 (Table 4) were taken from the same locations where in situ gamma and dose rate measurements were done (Figure 2), with the exception of T5, T22, T25, T26 and T29, where samples could not be obtained due to technical difficulties (problems with the approach and sampling), and T27 and T28, which are out of the zone of interest and therefore are not listed in the table. Samples marked as "Soil T-" were mostly soil-like material, hence the different label.

**Figure 3.** Laboratory for gamma spectrometry at the Institute for Medical Research and Occupational Health Laboratories, Zagreb, Croatia.

**Table 4.** Activity concentrations of K-40, U-238, Th-232 and Ra-226 in composite samples from 1 $m^2$ surfaces and 15 cm in depth (Bq/kg).

| Sample Label | K-40 | U-238 | Th-232 | Ra-226 |
|---|---|---|---|---|
| T1 | 60.96 ± 0.90 [3] | 25.40 ± 4.22 | 9.52 ± 1.11 | 19.94 ± 1.04 |
| T2 | 209.17 ± 1.45 | 28.81 ± 5.24 | 14.39 ± 0.831 | 26.45 ± 1.41 |
| T3 | 330.52 ± 2.06 | 37.71 ± 4.55 | 24.01 ± 0.69 | 36.31 ± 1.46 |
| T4 | 202.64 ± 2.94 | 33.07 ± 2.92 | 16.682 ± 0.9534 | 31.20 ± 1.83 |
| T6 | 232.82 ± 5.73 | 1721.00 ± 72.00 | 51.35 ± 3.11 | 1827.00 ± 19.00 |
| T7 | 97.82 ± 1.88 | 145.73 ± 11.96 | 17.09 ± 1.296 | 153.10 ± 3.20 |
| T8 | 160.32 ± 2.95 | 298.95 ± 25.00 | 19.96 ± 2.406 | 355.20 ± 5.50 |
| T9 | 306.90 ± 5.37 | 1049.15 ± 53.31 | 67.78 ± 1.95 | 1161.00 ± 14.83 |
| T10 | 244.41 ± 3.84 | 629.70 ± 48.24 | 49.42 ± 3.23 | 646.70 ± 10.01 |
| T11 | 296.50 ± 5.29 | 853.70 ± 71.67 | 52.91 ± 1.825 | 1004.00 ± 14.72 |
| T12 | 132.77 ± 1.86 | 216.40 ± 25.15 | 20.98 ± 1.44 | 218.80 ± 4.10 |
| T13 | 76.70 ± 2.65 | 190.07 ± 21.61 | 13.03 ± 1.90 | 158.60 ± 6.07 |
| T14 | 254.14 ± 5.87 | 1735.00 ± 76.40 | 54.49 ± 2.94 | 1759.00 ± 19.60 |
| T15 | 340.15 ± 3.85 | 205.23 ± 25.13 | 62.42 ± 2.50 | 161.73 ± 4.58 |
| T16 | 103.89 ± 3.45 | 948.20 ± 40.61 | 34.54 ± 1.64 | 681.70 ± 9.60 |
| T17 | 177.38 ± 3.63 | 474.99 ± 29.39 | 34.22 ± 2.92 | 551.69 ± 9.51 |
| T18 | 296.80 ± 4.20 | 23.96 ± 2.80 | 21.82 ± 2.32 | 43.14 ± 4.25 |
| T19 | 441.40 ± 6.41 | 1212.95 ± 76.91 | 96.14 ± 5.16 | 1257.62 ± 15.46 |
| T20 | 138.05 ± 3.28 | 882.20 ± 50.46 | 69.14 ± 6.10 | 809.65 ± 9.77 |
| T21 | 311.57 ± 7.57 | 1337.50 ± 80.00 | 60.24 ± 2.76 | 1430.00 ± 24.30 |
| T23 | 263.10 ± 6.24 | 1312.78 ± 123.24 | 87.22 ± 5.52 | 1301.72 ± 17.33 |
| T24 | 193.45 ± 4.03 | 1233.25 ± 66.74 | 73.98 ± 4.29 | 997.99 ± 11.95 |
| T30 | 303.62 ± 5.43 | 38.20 ± 3.09 | 24.65 ± 2.38 | 59.81 ± 4.75 |
| T31 | 239.49 ± 2.65 | 205.16 ± 21.97 | 21.81 ± 1.63 | 177.51 ± 3.86 |
| T32 | 149.86 ± 1.28 | 25.02 ± 8.15 | 8.32 ± 0.42 | 15.95 ± 1.07 |
| T33 | 197.27 ± 3.03 | 569.95 ± 44.99 | 31.74 ± 2.66 | 435.92 ± 7.33 |
| T34 | 232.03 ± 3.02 | 271.74 ± 33.68 | 28.14 ± 2.03 | 263.34 ± 5.64 |
| T35 | 148.26 ± 2.26 | 170.00 ± 18.00 | 15.08 ± 1.34 | 130.50 ± 5.40 |
| Soil T_1 | 251.14 ± 5.11 | 1219.00 ± 64.00 | 89.84 ± 4.49 | 1345.94 ± 28.60 |
| Soil T_4 | 238.30 ± 4.90 | 861.70 ± 76.24 | 52.77 ± 4.50 | 734.50 ± 12.44 |

[3] All values are given in (Bq/kg).

### *3.5. Laboratory Gamma Spectrometry Measurements of Activity Concentrations of Radionuclides from Exploratory Boreholes*

Three exploratory boreholes were drilled, and several samples (Figure 4) were taken for laboratory gamma spectrometry (Table 5), to determine activity concentrations of K-40, U-238, Th-232, and alpha spectrometry, for Ra-226 in depth.

**Figure 4.** Samples of coal ash and slag from exploratory boreholes.

**Table 5.** Activity concentrations of K-40, U-238, Th-232 and Ra-226 in samples taken from exploratory boreholes B2, B3 and B4 (Bq/kg) at given depths.

| Borehole Sample Label | Sampling Depth (m) | K-40 | U-238 | Th-232 | Ra-226 |
|---|---|---|---|---|---|
| B2-0 | 0.0 | 147.60 ± 4.15 [4] | 1265.45 ± 81.58 | 43.83 ± 3.76 | 957.21 ± 13.62 |
| B2-1 | 0.6 | 205.43 ± 8.41 | 1528.46 ± 128.65 | 34.69 ± 3.88 | 1290.51 ± 24.80 |
| B2-2 | 1.7 | 175.04 ± 6.83 | 1128.80 ± 111.10 | 32.09 ± 3.28 | 947.56 ± 24.42 |
| B2-5 | 4.8 | 104.95 ± 3.53 | 812.11 ± 99.93 | 40.49 ± 3.28 | 665.10 ± 10.39 |
| B2-6 | 5.6 | 212.52 ± 6.93 | 1719.33 ± 72.4 | 53.83 ± 3.27 | 1547.72 ± 23.20 |
| B2-7 | 6.6 | 135.35 ± 5.02 | 1257.26 ± 78.3 | 35.17 ± 2.22 | 1052.38 ± 16.13 |
| B2-10 | 9.9 | 23.20 ± 0.95 | 4.48 ± 0.74 | 1.69 ± 0.73 | 11.96 ± 2.03 |
| B2-11 | 10.8 | 144.51 ± 3.22 | 25.43 ± 3.15 | 7.07 ± 1.28 | 18.52 ± 2.19 |
| B2-12 | 11.8 | 132.98 ± 3.94 | 14.89 ± 4.87 | 7.00 ± 1.25 | 23.80 ± 2.86 |
| B2-13 | 12.9 | 219.48 ± 2.89 | 13.22 ± 1.14 | 11.53 ± 1.09 | 20.55 ± 2.12 |
| B3-2 | 1.75 | 295.18 ± 10.33 | 1134.22 ± 143.64 | 67.16 ± 8.54 | 790.30 ± 28.11 |
| B3-4 | 3.65 | 286.80 ± 11.96 | 1174.6 ± 128.49 | 74.83 ± 6.50 | 845.15 ± 25.35 |
| B3-6 | 5.8 | 147.29 ± 5.47 | 1224.43 ± 95.77 | 60.97 ± 5.06 | 1120.84 ± 18.92 |
| B3-7-0 | 6.35 | 171.73 ± 5.37 | 1417.16 ± 96.20 | 72.30 ± 4.55 | 1127.99 ± 17.07 |
| B3-8 | 7.6 | 233.74 ± 5.62 | 1361.98 ± 87.58 | 49.42 ± 4.51 | 948.26 ± 16.64 |
| B3-9 | 8.8 | 204.89 ± 6.86 | 1048.43 ± 103.18 | 45.09 ± 5.26 | 738.75 ± 18.28 |
| B3-10-0 | 9.3 | 150.66 ± 2.84 | 210.19 ± 14.42 | 31.71 ± 1.92 | 188.13 ± 4.09 |
| B3-10-2 | 9.5 | 76.78 ± 1.70 | 53.15 ± 8.89 | 5.06 ± 0.95 | 22.56 ± 2.28 |
| B3-10-3 | 9.85 | 122.71 ± 2.12 | 52.07 ± 18.23 | 9.56 ± 1.02 | 38.58 ± 2.58 |
| B3-11 | 10.8 | 186.95 ± 3.75 | 67.39 ± 19.04 | 9.84 ± 1.41 | 16.27 ± 2.42 |
| B4-3 | 2.65 | 267.88 ± 10.06 | 1290.19 ± 141 | 61.76 ± 7.15 | 932.55 ± 23.03 |
| B4-6-0 | 5.7 | 262.45 ± 7.21 | 1374.61 ± 85.93 | 70.68 ± 6.37 | 1257.16 ± 21.27 |
| B4-8-1 | 7.9 | 291.47 ± 8.63 | 1541.10 ± 153.74 | 88.88 ± 6.76 | 1396.00 ± 29.40 |
| B4-9 | 8.8 | 259.78 ± 7.43 | 1201.48 ± 112.88 | 64.30 ± 6.03 | 1158.52 ± 20.36 |

[4] All values are given in (Bq/kg).

The locations of boreholes, as shown in Figure 2, were selected with the aim of sampling coal ash and slag in areas where more significant concentrations of radionuclides are expected, considering the origin of the sampled material and the results obtained by the track method measurements of the surface ambient dose rate. Data from borehole B1 is not relevant to this research since it was drilled to determine only the geological composition of the soil. Borehole B1 was strategically positioned outside the primary contamination plume to serve as a regional reference (background) point for the site's geological characteristics. The entire study area is characterized by a uniform geological setting consisting of Eocene flysch deposits. Since lithology (alternating layers of sandstone and marl), with limestone as bedrock, is consistent across all sampled points, the geological data from B1 does not introduce any hidden variables that would alter the vertical distribution analysis of pollu-

tants. Instead, B1 confirms the regional geological structure, supporting the assumption of uniform transport conditions across the site.

It must be noted that the coal used for combustion in the power plant did not originate from only one mine but from different coal mines in the former SFRY [21–24], depending on availability. This, as well as the fact that hydro-transport of ash to the precipitate dumpsite was used, is the reason for the different concentrations of radionuclides by depth and on the surface.

### *3.6. Laboratory Gamma Spectrometry Measurements of Radon Exhalation Rates*

At the time of the research described in this paper, the radon (Rn-222) concentration in soil gas was not measured in situ. To determine the radon exhalation rates from the soils and coal ash and slag at the location, material samples (Figure 2) were analyzed in the laboratory via gamma spectrometry using the secular equilibrium time after the samples were prepared (Table 6). Sample Rn9 was damaged and hence discarded. The differences in the values of the radon exhalation rate can be attributed partly to the type of samples (soil, coal ash and slag, mixture of materials) and partly to ash and slag originating from different coals since the coal for the power plant was acquired from different mines in the former SFRY. Currently (the first quarter of 2026), extensive measurements of Rn-222 concentration in soil gas are performed on site using an AlphaGUARD Radon Monitor, Bertin Instruments, Montigny-le-Bretonneux. France, which will be considered during the discussion of the results.

**Table 6.** Results of laboratory gamma spectrometry measurements of radon exhalation rates ($Bq/m^2/h$).

| Sample Label | Radon Exhalation Rate ($Bq/m^2/h$) |
|---|---|
| Rn1 | $0.14 \pm 0.00$ |
| Rn2 | $0.01 \pm 0.00$ |
| Rn3 | $0.02 \pm 0.01$ |
| Rn4 | $0.02 \pm 0.00$ |
| Rn5 | $0.32 \pm 0.02$ |
| Rn6 | $0.82 \pm 0.02$ |
| Rn7 | $1.29 \pm 0.05$ |
| Rn8 | $0.55 \pm 0.02$ |
| Rn10 | $0.84 \pm 0.03$ |
| Rn11 | $1.49 \pm 0.05$ |
| Rn12 | $1.07 \pm 0.04$ |
| Rn13 | $0.55 \pm 0.03$ |
| Rn14 | $1.09 \pm 0.04$ |
| Rn15 | $0.81 \pm 0.03$ |
| Rn16 | $0.68 \pm 0.03$ |
| Rn17 | $1.15 \pm 0.06$ |
| Rn18 | $1.30 \pm 0.02$ |
| Rn19 | $0.77 \pm 0.03$ |
| Rn20 | $0.78 \pm 0.01$ |
| Rn21 | $0.82 \pm 0.02$ |
| Rn22 | $1.02 \pm 0.04$ |
| Rn23 | $1.47 \pm 0.10$ |
| Rn24 | $1.42 \pm 0.06$ |

### *3.7. Statistical Preprocessing, Geospatial Inspection of the Acquired Datasets and Map Development*

Prior to spatial analysis, all the abovementioned tabular datasets were subjected to quality control, statistical preprocessing and geospatial inspection. Extreme values that were identified as outliers or inconsistent with surrounding observations were removed prior to interpolation. Retained high values that exhibited spatial consistency were treated as valid indicators of localized contamination and preserved in the analysis.

Due to substantial differences among the analyzed variables, data standardization was required to enable meaningful integration of variables expressed in different physical units and value ranges, as well as assessment of combined environmental pressure from multiple contaminants. The minimum–maximum (Min–Max) standardization method was applied to three multivariable datasets (Tables 1, 3 and 4), transforming original values into a common range between 0 and 1 while preserving relative differences among observations. The standardized datasets were used for both correlation analysis and the generation of cumulative spatial maps. Pearson's correlation analysis was applied to explore intervariable relationships and to support the interpretation of spatial similarities observed in the interpolation maps. As an example, Table 7 presents the Pearson correlation matrix for heavy metal concentrations obtained using Statistica 14.0.0.15 software [45].

**Table 7.** Pearson's correlation matrix for heavy metal concentrations.

| **Correlations (Metals_Standardization)<br>Marked Correlations are Significant at $p < 0.01000$<br>N = 30 (Casewise Deletion of Missing Data)** | | | | | | | | | | |
|---|---|---|---|---|---|---|---|---|---|---|
| **Variable** | **Cd** | **Ni** | **Co** | **Cr** | **Tl** | **Pb** | **Mn** | **Cu** | **Zn** | **Fe** |
| Cd | 1.000 | | | | | | | | | |
| Ni | −0.446 | 1.000 | | | | | | | | |
| Co | −0.419 | 0.965 | 1.000 | | | | | | | |
| Cr | −0.123 | 0.735 | 0.663 | 1.000 | | | | | | |
| Tl | 0.341 | −0.583 | −0.508 | −0.414 | 1.000 | | | | | |
| Pb | −0.489 | 0.867 | 0.868 | 0.564 | −0.525 | 1.000 | | | | |
| Mn | −0.450 | 0.898 | 0.936 | 0.626 | −0.441 | 0.867 | 1.000 | | | |
| Cu | −0.429 | 0.916 | 0.943 | 0.559 | −0.448 | 0.846 | 0.872 | 1.000 | | |
| Zn | −0.470 | 0.948 | 0.980 | 0.616 | −0.560 | 0.934 | 0.918 | 0.941 | 1.000 | |
| Fe | −0.145 | 0.751 | 0.671 | 0.656 | −0.481 | 0.725 | 0.622 | 0.579 | 0.673 | 1.000 |

While the strong positive correlations observed between certain heavy metals suggest a common anthropogenic origin related to the site's former industrial activities, these statistical associations should be interpreted with caution. High correlation coefficients indicate similar spatial distribution patterns and geochemical behavior within the Eocene flysch, but they do not provide unequivocal proof of a singular source. Other factors, such as similar adsorption affinities to soil organic matter or iron oxides, may also contribute to these observed trends. Therefore, while the industrial history of the site remains the most plausible driver, the correlations serve as primary indicators of commonality rather than absolute source attribution.

The correlation structure presented in Table 7 provides important information on the sources and pathways of heavy metals. A significantly positive correlation at $p < 0.01$ was found between the elemental pairs Zn-Co (0.980), Zn-Ni (0.948), Zn-Pb (0.934), Zn-Mn (0.918), Zn-Cu (0.941), Cu-Ni (0.916), Cu-Co (0.943) and Co-Ni (0.965). Zn-Tl (−0.560), Pb-Tl (−0.525), Tl-Ni (−0.583) and Tl-Co (−0.508) are significantly (but less than in the case of a positive correlation) negatively correlated at $p < 0.01$. Two examples (since showing all maps would significantly increase the length of this paper) that visually confirm these significant correlations are the interpolated maps of Zn (Figure 5) and Co concentrations (Figure 6).

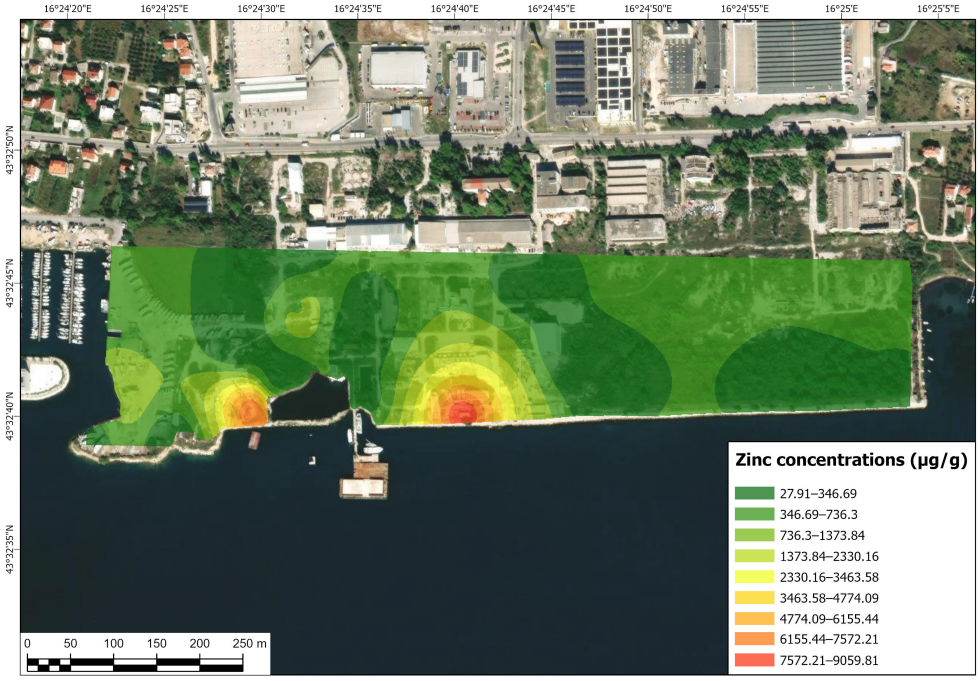


**Figure 5.** Interpolated map of Zn concentrations.

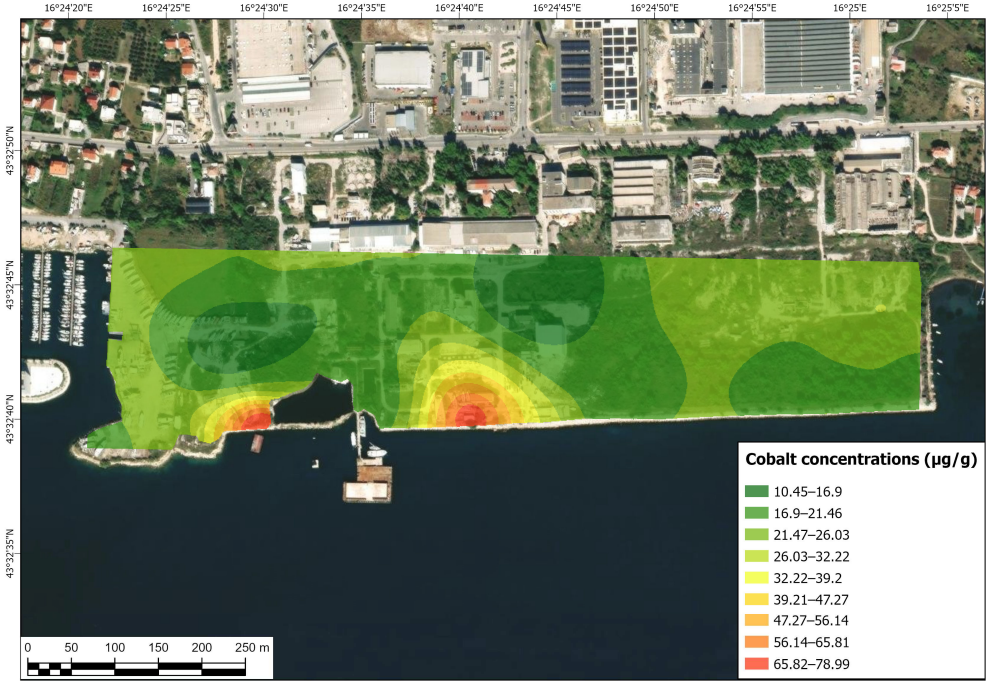


**Figure 6.** Interpolated map of Co concentrations.

The reasons for grouping (positive correlation) certain elements are related somewhat to the original industrial activities on site and partly, after the factory was closed, to the shipyard and shipbuilding activities from the 2000s to today. Coal storage before combustion in the power plant, and coal ash and slag disposal and spread, is moderately "responsible" for the distribution of Fe (pyrite) and Cd (present in rock samples as primary sphalerite) and partly for Ni (Ni-Fe sulfates and sulfides) and Cr (chrome-bearing spinels) due to composition and accessory minerals [46–53]. However, industrial activities related to shipbuilding have a significant effect on the presence of most heavy metals in the soil. The main reason for the specific distribution of thallium concentration is related to coal combustion in the local power plant [54,55].

The soil pollution maps of heavy metals generated by using GIS techniques help to analyze the distribution of all heavy metals—correlated heavy metal pairs—and it is easy to recognize graphical (geospatial) matching with Pearson's correlation matrix. For instance, the maps in Figures 5 and 6 look almost the same, which confirms strong positive correlations, whereas negative correlations between, e.g., Tl and Zn (Figures 5 and 7) show the opposite trend. Thus, whereas the value of Tl increases, the values of Zn, Ni and Pb decrease in terms of the concentration of heavy metal pollution in the soil.

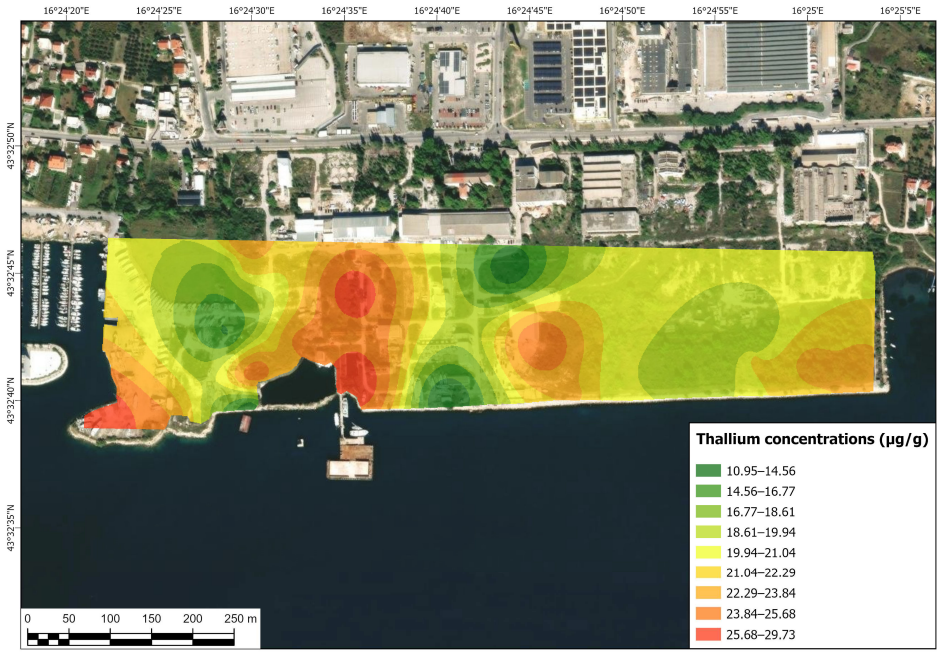


**Figure 7.** Interpolated map of Tl concentrations.

Sampling locations were georeferenced and integrated into a structured GIS database, together with relevant basemap layers. A regular grid with a spatial resolution of $1 \times 1$ m$^2$ was applied consistently across all interpolations to ensure spatial comparability between resulting raster layers. GIS functionality was used for data management, vector-based analysis, raster generation, and spatial overlay operations. Individual interpolation maps were produced for each contaminant variable, resulting in a total of 24 thematic maps, supplemented by four cumulative maps representing grouped contaminant categories.

All variables were spatially interpolated using Empirical Bayesian Kriging (EBK), a geostatistical method implemented in ArcGIS Pro 3.6.1 [56]. EBK was selected after analyzing all other common interpolation methods [57–61] for its ability to account for uncertainty in variogram estimation and its suitability for datasets with limited sampling density and heterogeneous spatial patterns. Unlike traditional kriging, which assumes a single global variogram, EBK subdivides the dataset into local subsets and estimates spatial dependence individually for each, improving prediction reliability and reducing bias—particularly in complex environmental datasets with non-uniform spatial variability. This method was applied uniformly to all datasets, including heavy metals, in situ and laboratory-measured radionuclides, dose rate values and radon concentrations, ensuring methodological consistency across all generated maps [62–64].

To evaluate cumulative contamination patterns, standardized EBK interpolation outputs were combined using raster algebra techniques. Three cumulative maps were generated: one representing heavy metal contamination, one representing in situ radionuclide distribution and one representing laboratory-determined radionuclide activities. These cumulative maps provide an integrated representation of overlapping contamination and

facilitate the identification of spatial hotspots characterized by elevated contaminant intensity. Excluded data points, after technical validation, contained incorrect geographic coordinates (placing them outside the study area) or incomplete analytical records. These were treated as invalid data entries rather than statistical outliers. Since the site is a former industrial facility, a conservative approach was chosen to identify statistical outliers representing high concentrations (potential hotspots) and retain them in the dataset, which ensured that the final spatial interpolation (EBK) and cumulative maps reflect the actual maximum contamination risks at the site. The accuracy of the spatial interpolation was validated using a leave-one-out cross-validation technique. Detailed interpolation accuracy metrics (ME, RMSE, and RMSS) for all 22 analyzed variables (heavy metals, radionuclides, and dose rates) are provided in Table S1 (Supplementary Material).

Figure 8 shows the interpolated map of all heavy metal concentrations, where higher values correspond to the locations of small shipyards and specific areas affected by the spread of certain elements during power plant activity.

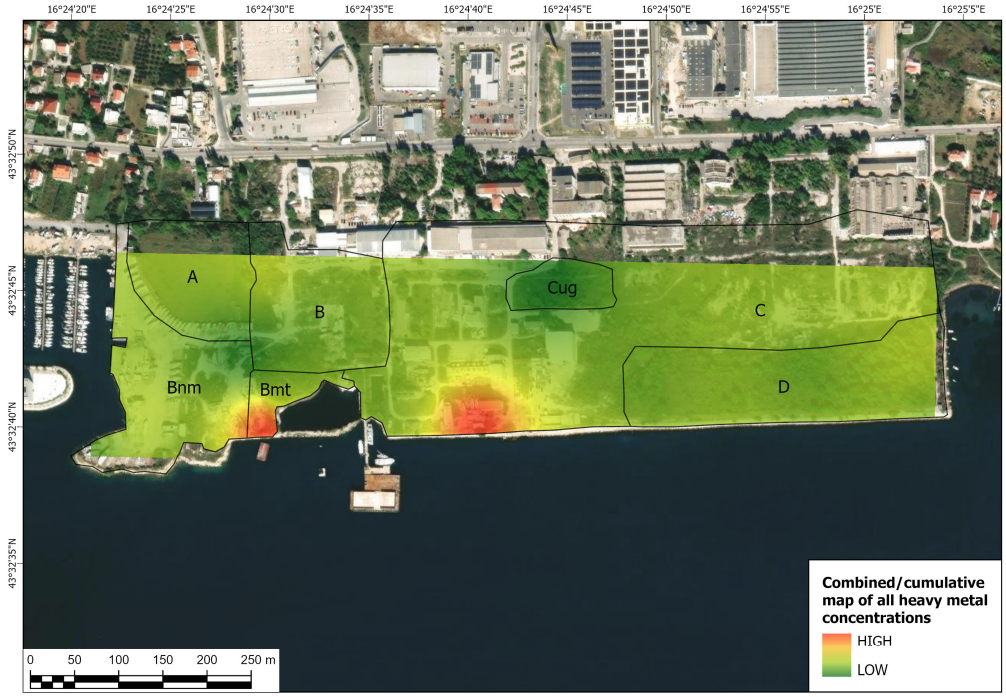


**Figure 8.** Interpolated map of all heavy metal concentrations (for zone designations, see Figure 2).

Dose rate measurement was organized according to the expected arrangement of NORM residues, where higher concentrations of radionuclides are expected, and the interpolated map (Figure 9) showed areas of interest for the following research (sampling and in situ measurements of radionuclide activity).

Maps created for specific radionuclides also show a positive correlation between radionuclides, which is evident for Pb-214 and Bi-214 (both belong to the U-238 decay chain, where Bi-214 is formed from the decay of Pb-214). There is a significant positive correlation (Figures 10 and 11) between Pb-214 and Bi-214 (0.980), which is also apparent in the maps for each of these radionuclides.

Cumulative concentrations of radionuclides in the soil at the considered site are shown in Figure 12, as an interpolated map of activity concentrations of Ra-226, Pb-214, Bi-214, Ac-228, Bi-212, Tl-208 and K-40 measured in situ, and Figure 13, as an interpolated map of activity concentrations of K-40, U-238, Th-232 and Ra-226 in composite samples taken at 1 $m^2$ surfaces from 15 cm in depth, prepared to reach secular equilibrium and then measured in the laboratory.

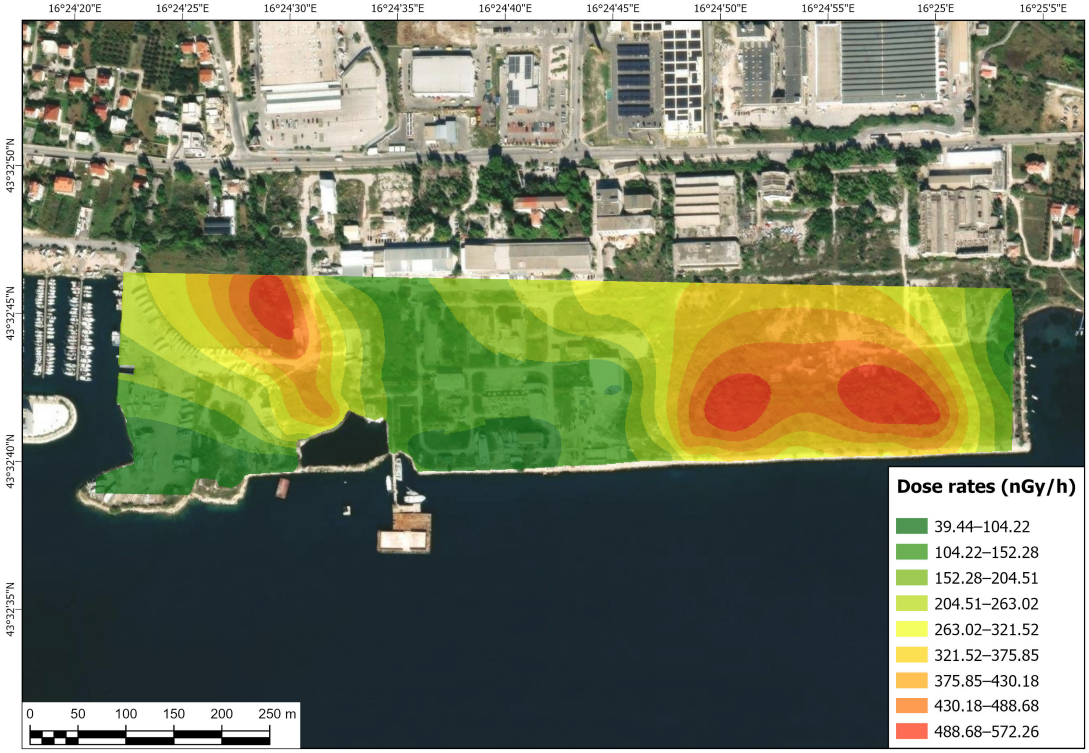


**Figure 9.** Interpolated map of dose rates.

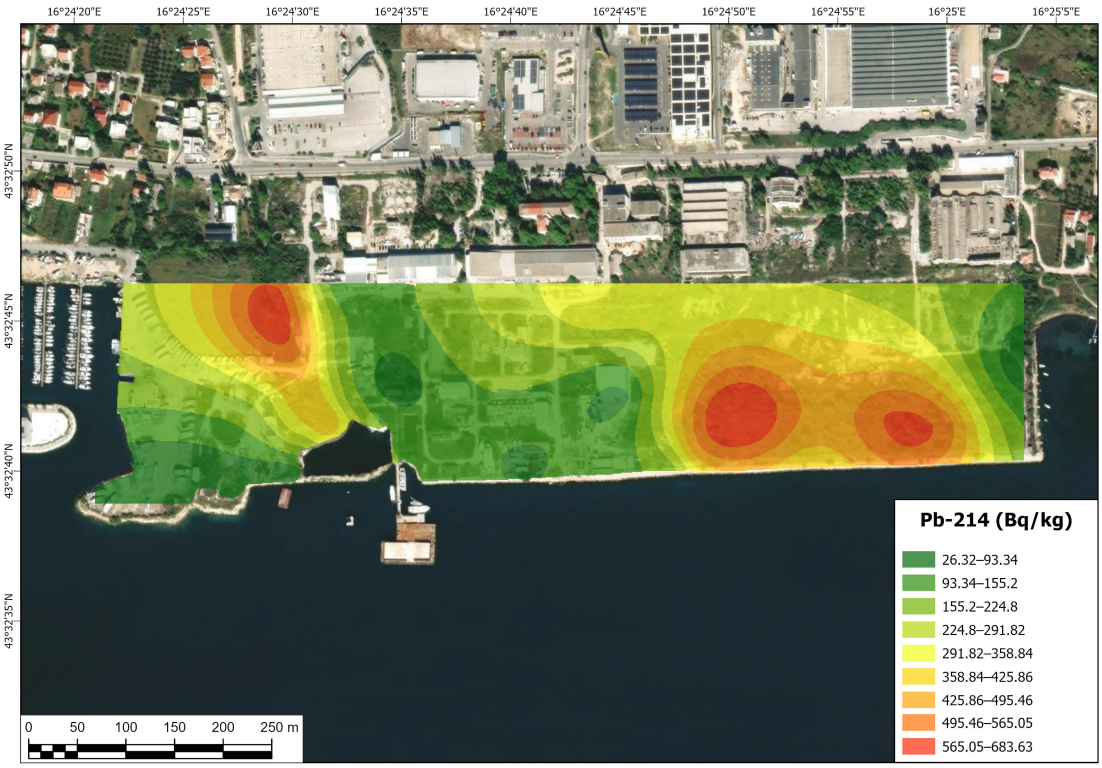


**Figure 10.** Interpolated map of activity concentrations of Pb-214 measured in situ.

https://doi.org/10.3390/su18083897

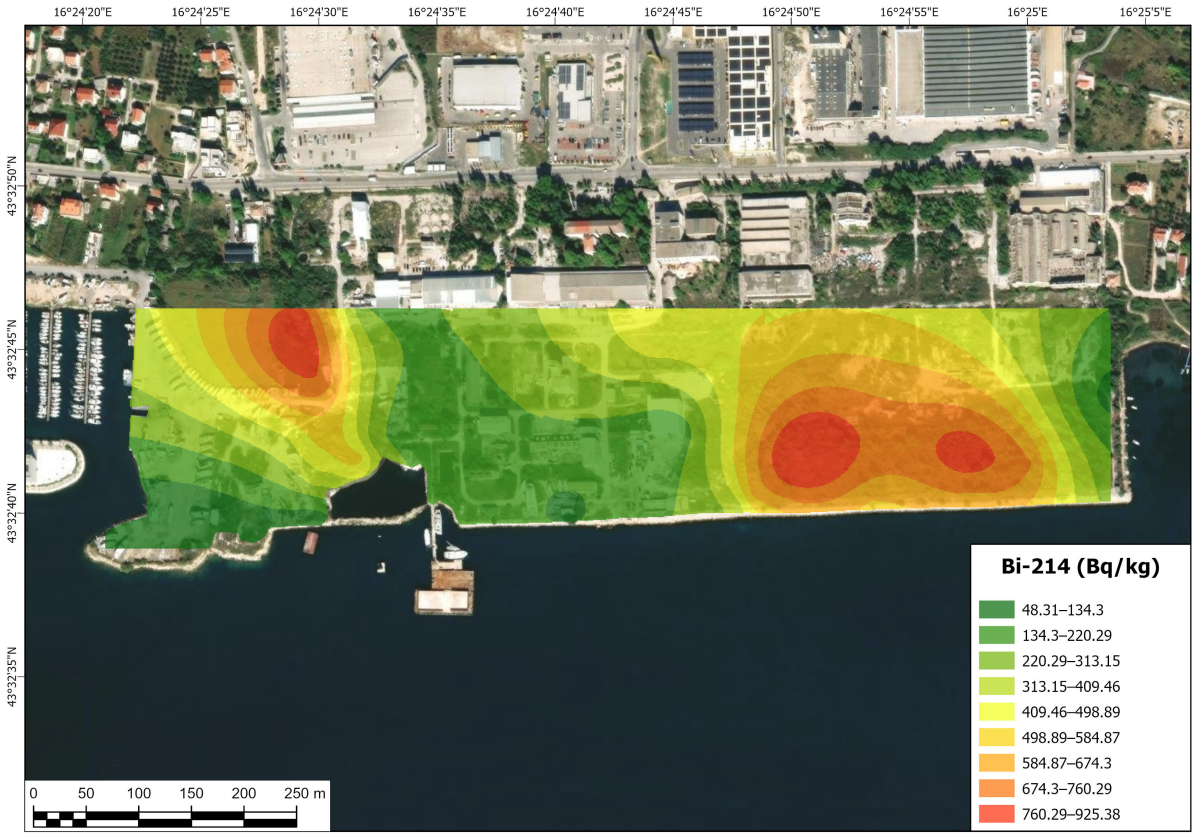


**Figure 11.** Interpolated map of activity concentrations of Bi-214 measured in situ.

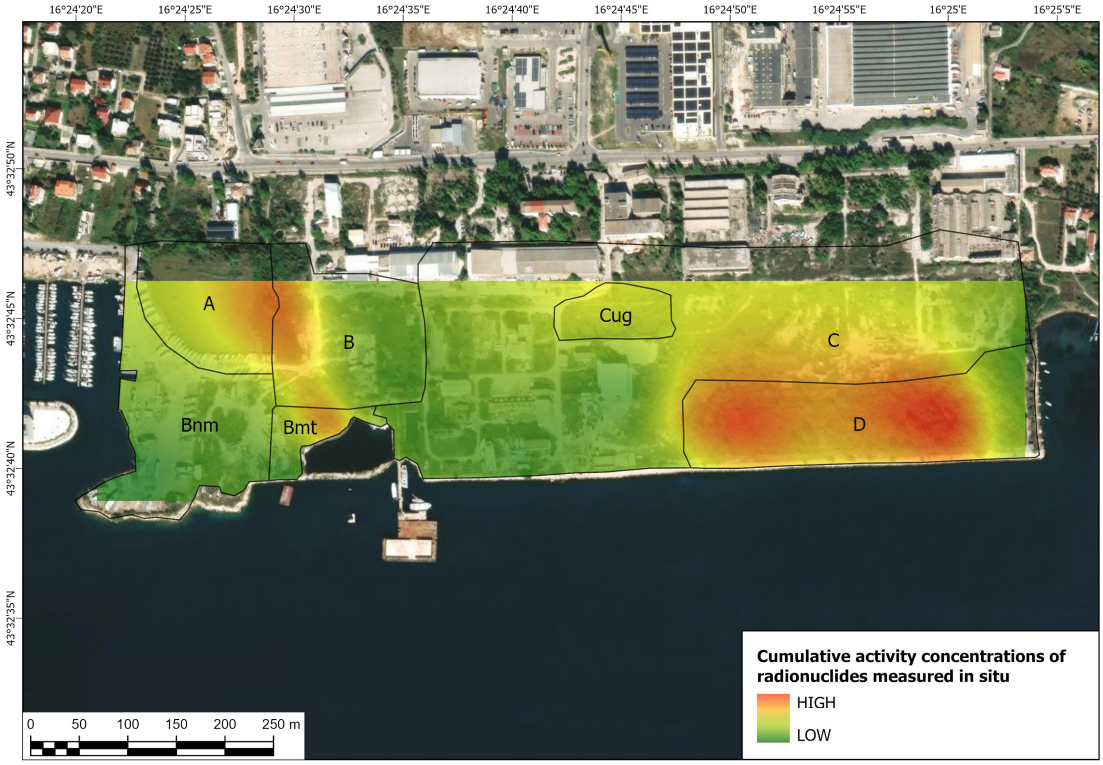


**Figure 12.** Interpolated map of activity concentrations of seven radionuclides Ra-226, Pb-214, Bi-214, Ac-228, Bi-212, Tl-208 and K-40 measured in situ (for zone designations, see Figure 2).

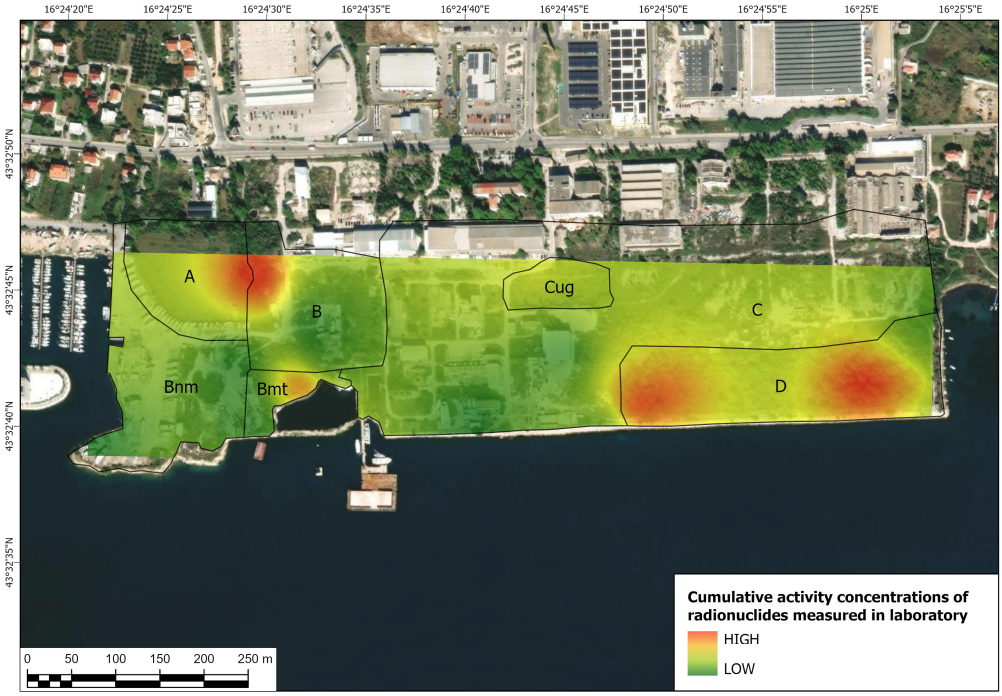


**Figure 13.** Interpolated map of activity concentrations of K-40, U-238, Th-232 and Ra-226 measured in the laboratory (for zone designations, see Figure 2).

Comparing the maps shown in Figures 12 and 13, the in situ and laboratory gamma spectrometry measurements of radionuclide activities indicate that areas with higher activity correspond to each other, although the same set of radionuclides was not analyzed. This is because high-resolution detectors (in situ gamma-ray spectrometers) used to identify radionuclides and measure their concentrations in soil from 1 m above the surface are programmed to identify radionuclides with higher energy outputs and, in certain cases, anthropogenic radionuclides. Laboratory measurements, on the other hand, are usually performed to identify and measure concentrations of primordial naturally occurring radionuclides and their significant progeny (e.g., Ra-226 due to its radiotoxicity). This fact is to be considered in every discussion of measured activities when dealing with NORM residues in the environment. The maps clearly show that higher concentrations of naturally occurring radionuclides correspond to industrial activities related only to coal ash and slag disposal—Zones "A", "D" and "Bmt". Also, although the values of radionuclide activity concentrations obtained by in situ measurements are lower than those measured from samples in the laboratory, the maps correspond to each other significantly. Therefore, in situ measurements can provide preliminary data for potential areas with higher concentrations of radionuclides at ex-industrial sites (brownfields) and point to zones where more intensive research (sampling and laboratory measurements) is needed. Considering the level of contamination, after as dense as possible ambient dose rate measurements using the tracking method, laboratory measurements are mandatory to assess the actual situation.

Since this brownfield site contains NORM residues (coal ash and slag) of parent materials (coals) that originated from different mines, it is important to determine the correct amounts of NORM residues with higher activity and especially the spatial (depth) distribution of pockets of ash and slag with higher activity concentrations. The nature of hydro-transport is also somewhat responsible for creating pockets with higher radionuclide concentrations and hence higher activity. Knowing the accurate spatial distribution of these pockets can be of great significance during the remediation of the site, either by identifying which material must not be disturbed or which must be excavated and removed from the site. This will also influence the final cost of site remediation. Although there are some

discrepancies in the detailed surface distribution of the deposited ash and slag, the most significant discrepancies are related to the specific depths of the NORM residues in investigation Zone D (Figure 2). Additional investigative activities are needed to reach the original terrain surface (limestone), as well as the level of the water line within the dumpsite.

A couple of preliminary exploratory boreholes were drilled, and the samples taken at depth provide a clearer picture of the distribution of contaminants by volume of material. This information will help the decision-making process when considering the selection of possible remediation technology. Data from Table 4 on the activity concentrations of K-40, U-238, Th-232 and Ra-226 in the samples taken from exploratory boreholes B2, B3 and B4 (Bq/kg) are shown in Figures 14–16.

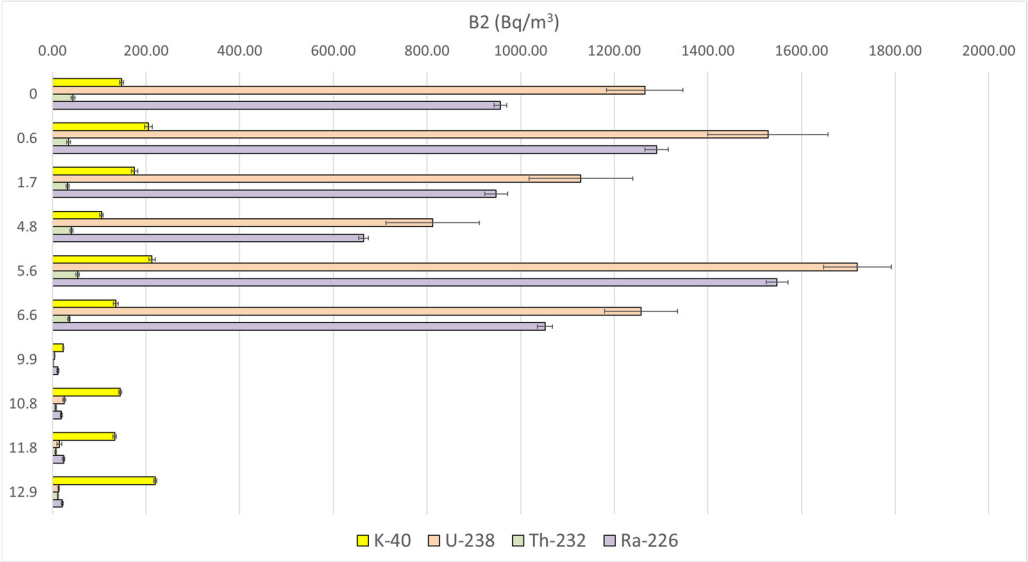


**Figure 14.** Activity concentrations of K-40, U-238, Th-232 and Ra-226 (Bq/kg) from exploratory borehole B2 by depth (m).

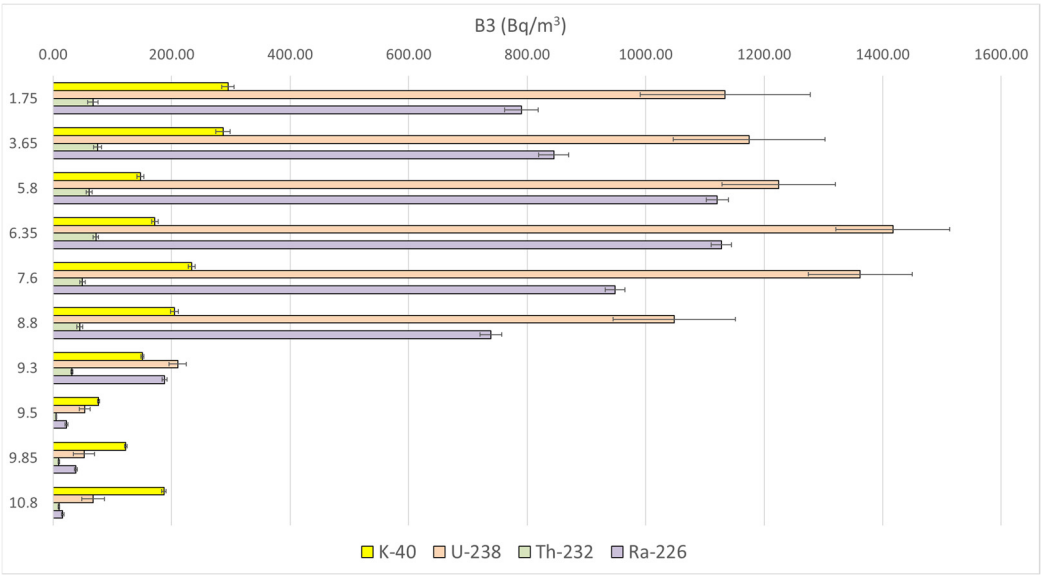


**Figure 15.** Activity concentrations of K-40, U-238, Th-232 and Ra-226 (Bq/kg) from exploratory borehole B3 by depth (m).

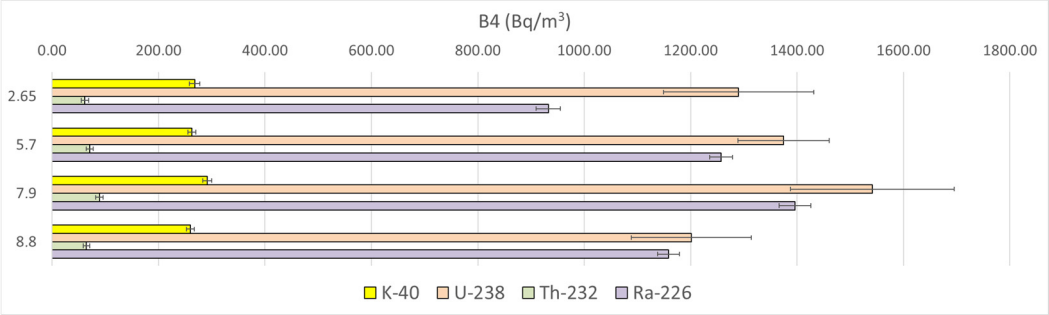


**Figure 16.** Activity concentrations of K-40, U-238, Th-232 and Ra-226 (Bq/kg) from exploratory borehole B4 by depth (m).

The discrepancy in the continuity of isotope concentrations in boreholes B-2 and B-3 (at the depth of ≈9 m) is related to the absence of a coal combustion residual deposit and the occurrence of clay minerals (soil) that are somewhat contaminated with ash and slag.

The radon (Rn-222) concentration in soil gas can indicate where higher concentrations of elements from the U-228 decay chain can be expected, and due to the relation between U-238 and U-235, the same is true for isotopes from the U-235 chain. The main reason for Rn-222 measurements is the possible exposure of people in the case of urbanizing a site containing NORM residues. A map of Rn-222 exhalation rates (Figure 17) in the soil samples from the location shows areas with higher emanation of Rn-222, but a more precise map is expected after ongoing research in which radon concentrations in soil/coal ash and slag will be measured in situ.

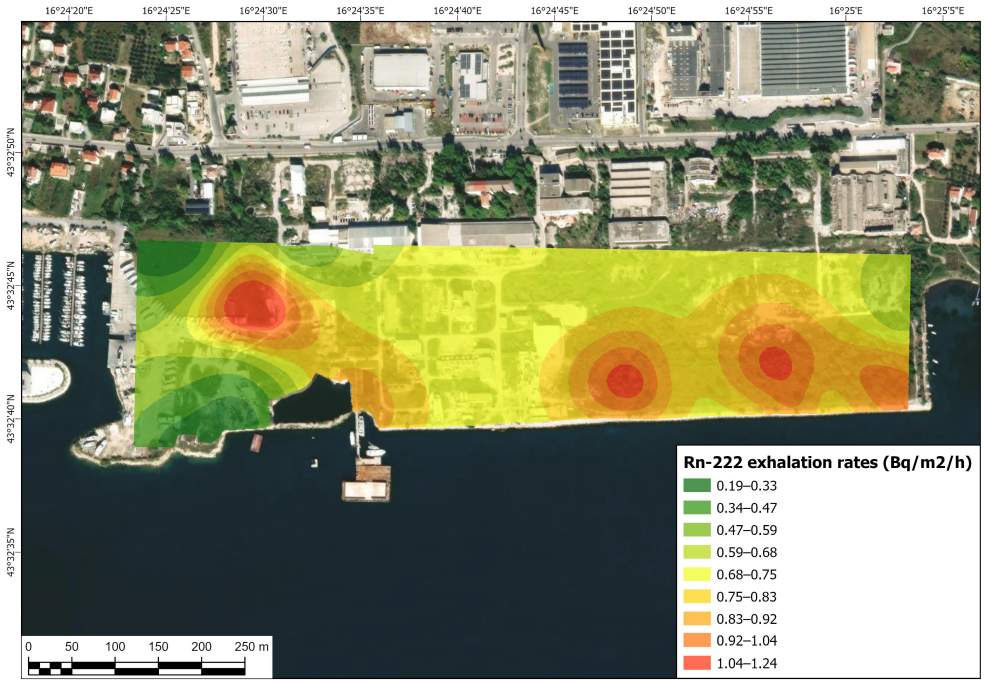


**Figure 17.** Interpolated map of Rn-222 exhalation rates measured from samples in the laboratory.

In this research, special interest was given to Ra-226 since it is a highly radiotoxic, naturally occurring, long-lived ($t_{1/2}$ = 1600 ± 7 years) α emitter (undergoes α decay to Ra-222) that emits significant γ radiation as well. Radiological risk assessments for NORM residue disposal sites [65–68] usually point to Ra-226 as the dominant contributor to dose rates in biota. As a primary "dose driver", Ra-226 contributes significantly to internal α dose, which can represent 72% to 97% of the total dose in some terrestrial ecosystems. Its progeny, Rn-222 gas, also an α emitter, is considered a major health hazard that, in normal

circumstances (not elevated concentrations), accounts for approximately 50% or more of the total radiation dose (both natural and man-made) received by the general population annually. When comparing the interpolated map of activity concentrations of Ra-226 measured in situ—above ground (Figure 18)—with the map of activity concentrations of Ra-226 measured in soil samples in the laboratory (Figure 19), the discrepancies and differences are explained by weathering and, hence, differences in concentrations and activities.

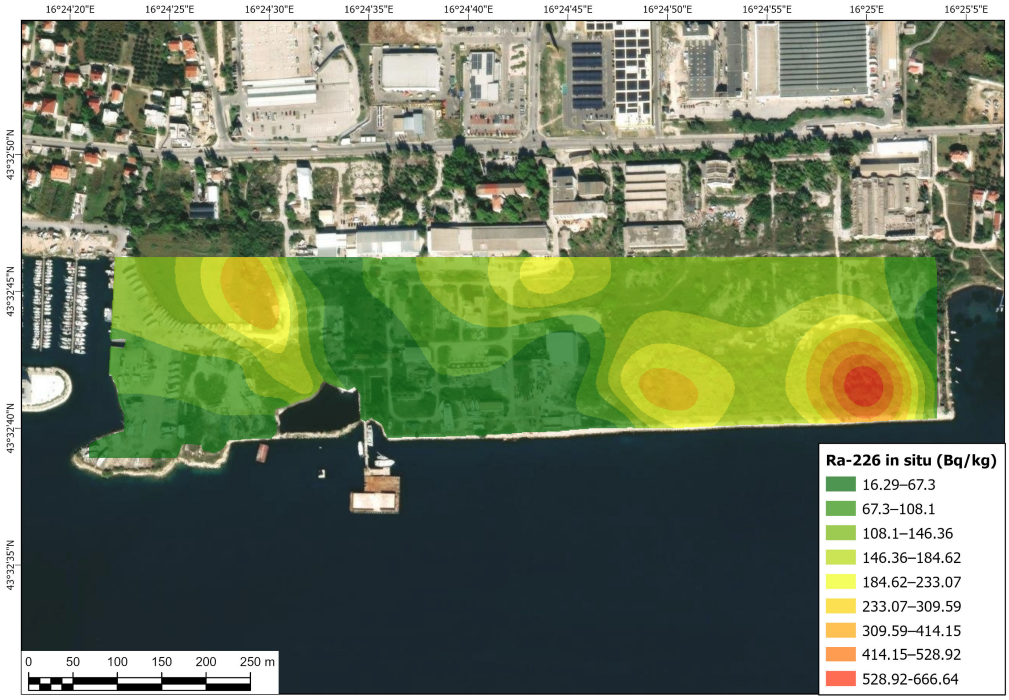


**Figure 18.** Interpolated map of activity concentrations of Ra-226 measured in situ.

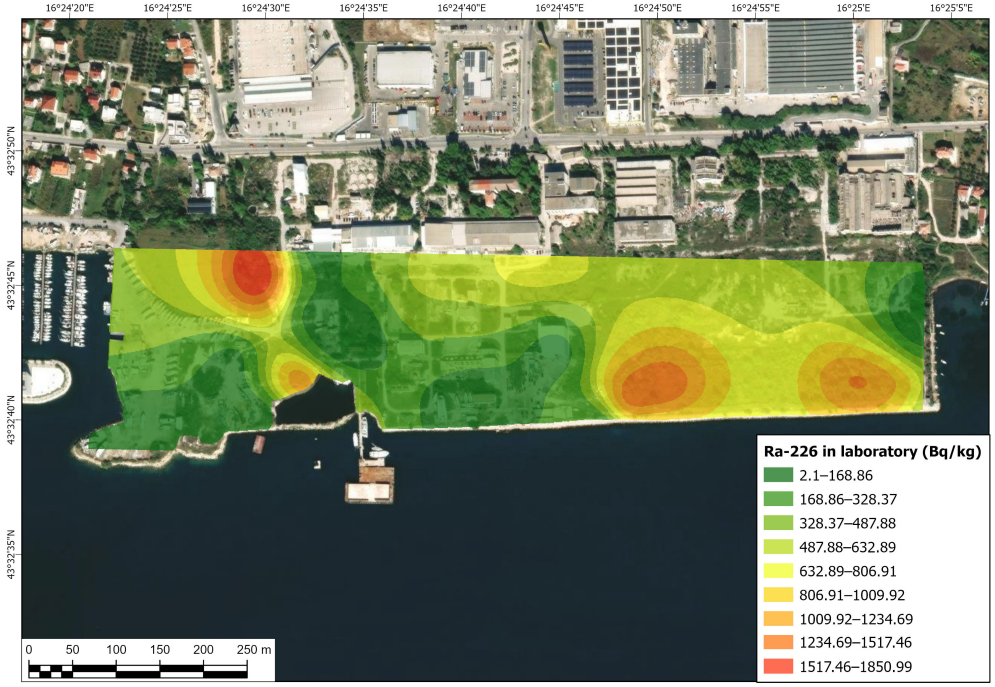


**Figure 19.** Interpolated map of activity concentrations of Ra-226 measured in the laboratory.

However, the maps do correspond to each other, and compared to an interpolated map of activity concentrations of Rn-222 (Figure 17), there is also an obvious relation. Differences

in the maps showing Ra-226 and Rn-222 concentrations are explained by: sampling for laboratory measurements of Ra-226 and Rn-222 at different locations, movements of Rn-222 gas through soil and laboratory measurement instead of in situ measurement of Rn-222 concentration in soil gas.

## 4. Discussion

One of the questions addressed in this research is whether the concentrations of heavy metals in the soil of Kaštela Bay represent a serious problem. Another question is what kind of additional, originally not planned, remediation of the site is required regarding additional and uncontrolled pollution due to intense small shipyard activity at the site, if it is to be repurposed, urbanized, or greened—i.e., made less harmful to the environment.

Although this location was not and is not planned to become an agricultural area, no existing Croatian regulatory document addresses any other type of land use related to heavy metal reference levels (maximum permitted concentrations), except for the one concerning agricultural land. Therefore, values taken from the Croatian Ordinance on protection of agricultural land from pollution [69] were used purely as comparison values, as shown in Table 8. It should be noted that values from the Ordinance are used for reference only as a conservative benchmark, since the site is intended for tourism, and these limits provide a higher safety margin compared to urban or industrial soil guidelines, which are not yet defined in Croatian regulatory documents.

**Table 8.** Maximum permitted amounts of heavy metals in agricultural soil in Croatia [69] (mg/kg).

| Element | Soil pH in 1 M KCl Solution | | |
|---|---|---|---|
| | <5 (mg/kg) | 5–6 (mg/kg) | >6 (mg/kg) |
| Cd | 1 | 1.5 | 2 |
| Cr | 40 | 80 | 120 |
| Cu | 60 | 90 | 120 |
| Hg | 0.5 | 1 | 1.5 |
| Ni | 30 | 50 | 75 |
| Pb | 50 | 100 | 150 |
| Zn | 60 | 150 | 200 |
| Mo | 15 | 15 | 15 |
| As | 15 | 25 | 30 |
| Co | 30 | 50 | 60 |

According to the Ordinance, agricultural land is considered polluted when it contains more heavy metals and potentially polluting elements than the maximum permitted amount (MPA), expressed in mg $kg^{-1}$ of air-dry soil. If the location is to be urbanized or remediated by landscaping and creating a promenade, the above table can be considered, but after the local flora was analyzed, the conclusion was that heavy metals do not affect the growth and health of autochthonous Dalmatian flora. Therefore, if material found on the site is not removed to another location during remediation but, for example, leveled and covered with humus during landscaping activities, heavy metal concentrations should not be of significant concern.

On the other hand, regarding possible remediation by means of civil construction at Zone "D" (Figure 2), the Croatian Ordinance on environmental monitoring of radioactivity [70] is to be consulted. It states: "*If the assessment of workers' exposure determines that workers may receive an effective dose of more than 1 mSv and less than 6 mSv in a year, the user of the industrial facility must take measures to reduce workers' exposure to as low a level as is reasonably achievable, taking into account technical, organizational, economic, health and social factors, inform these workers about the possible risks of exposure to ionizing radiation and provide them with access to the assessment. If it is estimated that workers may receive an effective*

*dose exceeding 6 mSv per year, the user of the industrial facility shall ensure the determination of the personal exposure of workers and periodic health checks and shall take measures to reduce the exposure of workers to as low a level as is reasonably achievable, taking into account technical, organizational, economic, health and social factors. If the measures do not allow the exposure of workers to be reduced below 6 mSv per year, these workers shall be considered exposed workers of category A.*"

A calculation of the effective dose for people exposed to ionizing radiation is shown in Table 2. "Dose rates measured on location (nGy/h)" shows that the highest measured dose rate (607.699 ± 0.77955 nGy/h) corresponds to the effective occupational dose to a worker of 1.217 mSv/y under the condition of 2000 working hours per year [71]. The value of 2000 working hours is chosen to represent a conservative "occupational scenario" for a full-time site employee (e.g., maintenance or security staff) spending 40 h per week outdoors for 50 weeks per year (with an occupancy factor of 1.0) during that period. A more realistic occupational scenario would imply significantly fewer working hours in zones of the considered area where a higher effective dose for workers exposed to elevated concentrations of radionuclides is expected. Considering a public (tourist) exposure scenario, assuming a representative stay of 168 h/year (3 weeks) with an outdoor occupancy factor of 1.0 during that period, the dose for tourists would be 0.1 mSv/period or less with a lower occupancy factor (e.g., a 0.2 occupancy factor for a short-term visitor dose would be 0.02 mSv/period). It has to be noted that these values are conservative, and expected doses should be lower after remediation of this location.

The calculation of the effective dose for workers exposed to elevated concentrations of Ra-226 in soil is based on the calculation of the absorbed gamma dose rate in air (nGy/h) at 1 m above the ground surface using the conversion factor of 0.462 nGy/h per Bq/kg of Ra-226 [72–75], assuming complete decay chain equilibrium, including Bi-214 and Pb-214. To calculate the total dose, the calculated dose must be combined with other primordial radionuclides (Th-232 and K-40) and properly integrated. The total dose rates have been found, for most of the area, to be below the conservative screening benchmark of 10 μGy/h, a value predicted to be the no-effect dose rate.

The radionuclide concentrations were compared with the IAEA GSR Part 3 Radiation Protection and Safety of Radiation Sources: International Basic Safety Standards [76], table I.3 of GSR Part 3. These standards ensure that "*Levels for clearance of material: activity concentrations of radionuclides of natural origin, do not exceed activity concentration of 10 Bq/g for K-49, and 1 Bq/g for each radionuclide in the uranium decay chain or the thorium decay chain*". Given the above, areas where excessive activity concentrations of specific radionuclides are observed must be avoided as potential areas for urbanization or any other human activity that would cause additional exposure. To ensure the avoidance of additional exposure and additional doses, certain locations must undergo specific remediation. Also, locations with higher activity concentrations cannot be disturbed by any remediation activity, nor can the material be excavated and transported from the location.

Data in Tables 3–5, as well as in Table 2, indicate higher levels of activity concentrations and dose rates related to radionuclides, corresponding to expected values for locations containing NORM residues. The values do not point to a serious problem related to human health, but they do indicate that urbanization of this location, which would include certain amounts of excavated and removed materials for the grounding of construction, is not a feasible option. Therefore, the existing plans for the construction of a five-star tourist complex on the wider area of this site must be accompanied by a proper risk assessment study. The maps in Figures 10–12, 18 and 19 indicate areas of specific concern that should be avoided as the potential zones for urbanization. However, they can still be considered as useful if properly remediated because only the surface of a small depth is affected in all

areas of concern, except at dumpsite "D" and partly at location "Bmt". The concentrations of Rn-222 also suggest that there would be a serious issue if living or enclosed working places were constructed in the "red areas".

Only specific contaminant maps with data shown in relation to regulatory documents, which define permitted amounts of certain contaminants, must be considered during decision-making related to selecting the exact areas to be remediated and the remediation technology that should be applied. Three cumulative maps (heavy metal contamination, in situ radionuclide distribution and laboratory-determined radionuclide activities) present the contamination at the considered brownfield site, which will assist decision-makers and stakeholders in general. The data presentation will vary depending on the expertise of stakeholders—from general to specific—with all data and visualizations available as needed. The created maps serve to both reduce concern for a brownfield site, which has long been considered "lost" due to pollution by some stakeholders, and show that not the entire location but only certain areas can be urbanized, as considered by other stakeholders.

Given the heterogeneous datasets and limited sampling locations, GIS served not only as a visualization tool but also as the core environment for spatial modeling, statistical preprocessing, and cumulative mapping. Interpolation maps reveal distinct spatial patterns for individual contaminants, highlighting both localized anomalies and broader trends. Certain areas consistently exhibit elevated values across multiple variables, reflecting heterogeneous distributions of heavy metals and radionuclides.

Cumulative maps effectively summarize the spatial coincidence of mixed contaminants, with heavy metal and radionuclide maps respectively highlighting hotspots and clusters corresponding to site characteristics. Visual comparison of individual maps confirms spatial correspondence between variables with statistically significant correlations, supporting the consistency of numerical correlation analysis and spatial modeling. High-resolution interpolation surfaces allow precise delineation of hotspots and transition zones, providing a detailed framework for environmental interpretation and risk assessment.

Dictated by the regulating authority's decisions and repurpose plans for this brownfield location, precise remediation techniques, if needed, will be chosen [77]. If urbanization is decided, the problem of constructing buildings or any other facility that needs deep excavation and foundations constructed on coal combustion residuals will raise (from a geotechnical engineering standpoint) the issue of disposing the excavated material. Any removal of combustion residuals from Zone "D" is not reasonable because then the excavated material has to be disposed of in a new special repository at another location, which is considered as the most expensive and most environmentally unsafe solution. No agricultural plans exist so far for the brownfield location in Kaštela Bay; therefore, heavy metal contamination will not represent an issue with regard to the cultivation of vegetation for the pure greening of the location. Anticipated site development will incorporate the erection of structures towards the back of area "D", inland, and landscaping the greater part of area "D", introducing textural variety by incorporating multi-stemmed specimens and woody foliage, the promenade, etc., with indigenous plant species, which are the most suitable from an ecological perspective. An alternative solution would be constructing a photovoltaic power station (solar park) since Kaštela Bay has between 2670 h and 2700 h of annual sunshine (according to data from the Croatian Meteorological and Hydrological Service [78]). The idea of using this site partially as a small craft harbor and docking area must be reconsidered or even abandoned, since the construction of infrastructure and supporting facilities would cause significant disturbance and significantly impact the deposited materials at the location.

Due to contemporary policies related to renewable energy, ground-mounted solar installation is a realistic possibility for this location. This would require the construction of a

layer of soil material covering most of Zone "D", as well as the construction of concrete pads and other similar activities. All this work must undergo scrutiny based on a risk assessment study developed specifically for every remediation, repurposing or construction plan. If material in Zone "D" will not be disturbed, some nautical facilities may still possibly exist at the external (toward the sea) border of Zone "D".

The important issues that must be pointed out are:

- Ensuring the safety of the regulated NORM residue disposal site in Kaštel Gomilica (Zone "A", in Figure 2), which must not be disturbed and probably will include additional cover, fencing off the area and preventing people from accessing it.
- Reducing existing fear and removing the stigma of a "radioactive location" from this location through scientific research publications, as well as other more adjusted types of communication with stakeholders, especially with the local community.

The first issue is technically feasible, although special scrutiny and attentive engineering activities must be applied. The second issue can take some time, but it can be addressed simultaneously with remediation, landscaping and other selected activities that have to be and can be done at this site. Hence, using the maps of contaminant spatial arrangements, it is possible to plan all the needed activities and select a final reasonable reuse of this ex-industrial site.

## 5. Conclusions

Remediation of old industrial sites with complex pollution conditions requires multifaceted research to identify which type of contaminant is present in which area and which industrial activity it is associated with. This enables easier decision-making concerning the way to conduct additional research, if needed, and the method and technology to remediate the area. In some cases, e.g., if the "polluter pays" principle is applied, identifying areas with specific contamination will help to resolve financing issues. This is important, especially in the case of locations with long-term legacy contamination from past industrial activities of different types, or the combination of inherited and recent industrial contamination.

The location of the decommissioned factory of plastics and chemical products, Jugovinil, City of Kaštela, Croatia, recently became an important area of interest since it is located right on the seashore and has a high potential for urban development and the establishment of tourist facilities. Except for NORM residues, i.e., coal combustion residuals originated from the power plant constructed for the ex-Jugovinil factory, contamination in this area is related to small shipyards active in the last three decades. The last, but certainly not least, issue related to this site represents the regulated NORM residue repository (Zone "A") bordering this area. To determine contaminated zones, types and concentrations of contaminants, extensive research was conducted, and the results are presented in contamination maps.

Current and planned further research on this location include: screening topographic features of terrain and monitoring vegetation using a drone, in situ extensive measurements of Rn-222 concentration in soil gas, additional surface and borehole sampling, geotechnical investigations of materials and the development of a 3D model of Zone D—the coal ash and slag precipitate dump site (Figure 2). This research and investigative work are necessary to properly plan the remediation of the site.

Zones with elevated concentrations of radionuclides are not to be disturbed, and remediation techniques that can be applied can only include leveling the terrain without relocating materials, applying a covering layer of inert soil material from the area where the site is located (thickness and composition of the material to be defined after further research), etc. Covering material must provide efficient protection from the population (workers,

tourists. . .) related to the absorbed dose rate, as well as a base for specific remediation (greening or construction of solar panels, for example). The current research results indicate that certain areas with higher concentrations of radionuclide activities in the coal ash and slag deposited at Zone "D" specifically are not suitable for the construction of buildings for accommodation or work, mainly due to potential radon exhalation into buildings and the resulting exposure. Specific areas where the construction of buildings, infrastructure and supporting facilities are not recommended are identified on maps showing the distribution of radionuclides (mainly Ra-226 and Rn-222) at the location. The maps also show which areas are not to be disturbed (regulated NORM repository, Zone "A") and which areas are to be covered with topsoil, thus remediating them by landscaping and planting grass, bushy plants and small trees, regarding the possible length of roots and the depth/thickness of cover material, at Zone "D". The probable part of the site repurposed by constructing a solar park also implies partly covering those areas with soil rather than simply leveling, and thus disturbing, the contaminated material.

This study demonstrates the effectiveness of integrating GIS and geostatistical methods for the spatial assessment of complex environmental datasets needed for the remediation of brownfield sites. Standardized interpolation and cumulative mapping enabled the comparison of heavy metals and radionuclides, highlighting hotspots and areas of overlapping contamination. Correlation analysis and spatial patterns were consistent, revealing co-occurrence and divergence not evident from numerical data alone. Integrating physical, ecological, and radiological information provides a comprehensive understanding of contaminant dynamics, potential ecological impacts, and radiological exposure. The multi-map approach offers both detailed local analysis and an overall assessment of cumulative environmental pressure, supporting informed decision-making and site management.

Since this study specifically considers the occurrence of heavy metals and NORM residues, in addition to its geographical position and probable future repurposing, it should be questioned whether the methodological framework used in this study can be used for the assessment of other brownfield sites. Brownfield sites usually include abandoned urban areas, landfills and disposal sites, areas contaminated during the transport of hazardous materials, abandoned military sites, former industrial zones, mines, oilfields, and mineral processing sites; most of these locations or areas can be surveyed using the methodological framework presented in this paper. Although the types and properties of contaminants can vary, if potential contaminants are properly identified and a survey of the location is carried out accordingly, the integration of GIS and geostatistical methods can be used to identify areas with specific conditions, areas with increased pollutant loads and/or "multiple stressors" can be singled out, and potential correlations between the concentrations of different contaminants can be observed. Maps, such as those presented in this paper, can help decision-makers define management of brownfield sites, decide on remediation methods, etc., bearing in mind that in order to solve problems in some locations, one should also have a three-dimensional distribution of contaminants.

**Supplementary Materials:** The following supporting information can be downloaded at https://www.mdpi.com/article/10.3390/su18083897/s1: Table S1: Geostatistical cross-validation metrics for Empirical Bayesian Kriging.

**Author Contributions:** Conceptualization, Ž.V. and D.P.; methodology, I.P.; software, D.P.; validation, Ž.V., D.P. and I.P.; formal analysis, D.P.; investigation, I.P.; data curation, I.P.; writing—original draft preparation, Ž.V.; writing—review and editing, Ž.V., D.P. and I.P.; visualization, D.P.; supervision, I.P. All authors have read and agreed to the published version of the manuscript.

**Funding:** This research received no external funding.

**Institutional Review Board Statement:** Not applicable.

**Informed Consent Statement:** Not applicable.

**Data Availability Statement:** Data will be made available on request.

**Acknowledgments:** The authors would like to thank the Institute for Medical Research and Occupational Health, Zagreb, Croatia, for part of the data collection and equipment use.

**Conflicts of Interest:** The authors declare no conflicts of interest.

## Abbreviations

The following abbreviations are used in this manuscript:

| | |
|---|---|
| EBK | Empirical Bayesian Kriging |
| GDP | Gross Domestic Product |
| GIS | Geographic Information System |
| IAEA | International Atomic Energy Agency |
| IMROH | Institute for Medical Research and Occupational Health, Zagreb, Croatia |
| MPA | Maximum Permitted Amount |
| NORM | Naturally Occurring Radioactive Materials |
| SFRY | Socialist Federative Republic of Yugoslavia |

## References

1. Kumari, S.; Mishra, A. Heavy Metal Contamination. In *Soil Contamination—Threats and Sustainable Solutions*; Larramendy, M.L., Soloneski, S., Eds.; IntechOpen: London, UK, 2021; pp. 1–14. [CrossRef]
2. Su, C.; Jiang, L.; Zhang, W. A review on heavy metal contamination in the soil worldwide: Situation, impact and remediation techniques. *Environ. Skept. Crit.* **2014**, *3*, 24–38.
3. Sudarningsih, S.; Fahruddin, F.; Lailiyanto, M.; Noer, A.A.; Husain, S.; Siregar, S.S.; Wahyono, S.C.; Ridwan, I. Assessment of Soil Contamination by Heavy Metals: A Case of Vegetable Production Center in Banjarbaru Region, Indonesia. *Pol. J. Environ. Stud.* **2023**, *32*, 249–257. [CrossRef]
4. Dunca, E.-C.; Ioniță, M.-F.; Radu, S.M. Soil Contamination and Related Ecological Risks: Complex Analysis of the Defor Petrila Tailings Dump, Romania. *Land* **2025**, *14*, 1492. [CrossRef]
5. Abdullahi, A.; Lawal, M.A.; Salisu, A.M. Heavy metals in contaminated soil: Source, accumulation, health risk and remediation process. *Bayero J. Pure Appl. Sci.* **2021**, *14*, 1–12. [CrossRef]
6. Rahman, R.O.A.; Elmesawy, M.; Ashour, I.; Hung, Y.-T. Remediation of NORM and TENORM contaminated sites-Review article. *Environ. Prog. Sustain. Energy* **2013**, *33*, 588–596. [CrossRef]
7. Peroni, M.; Mulas, V.; Betti, E.; Patata, L.; Ambrosini, P. Decommissioning and Remediation of NORM/TENORM Contaminated Sites in Oil and Gas. *Chem. Eng. Trans.* **2012**, *28*, 181–186. [CrossRef]
8. Waggitt, P.W. A Global Overview of NORM Residue Remediation and Good Practice. In *Proceedings of the 6. International Symposium on Naturally Occurring Radioactive Material (NORM VI)*; International Atomic Energy Agency: Vienna, Austria, 2011; pp. 311–326.
9. König, C.; Drögemüller, C.; Riebe, B.; Walther, C. Remediation of TENORM residues: Risk communication in practice. *J. Radiol. Prot.* **2014**, *34*, 575–593. [CrossRef]
10. *Statistical Information 2025*; Report; Croatian Bureau of Statistics: Zagreb, Croatia, 2025; Available online: https://podaci.dzs.hr/media/uxunslhk/statisticke-informacije-2025.pdf (accessed on 5 February 2026).
11. *Tourist Arrivals and Overnight Stay in 2025*; Report TUR-2023-1-2; Croatian Bureau of Statistics: Zagreb, Croatia, 2024; Available online: https://podaci.dzs.hr/media/0p4pjimd/tur-2025-1-1_11-dolasci-i-no%C4%87enja-turista-u-komercijalnom-smje%C5%A1taju-u-2025.pdf (accessed on 5 February 2026).
12. Environmental Pollution Register. Available online: https://envi-metapodaci.azo.hr/geonetwork/srv/hrv/catalog.search#/metadata/195db58e-d265-4892-b5a2-3937cb89214e (accessed on 5 February 2026).
13. Croatian Parliament. *The Radioactive Waste, Disused Sources and Spent Nuclear Fuel Management Strategy*; Official Gazette: Zagreb, Croatia, 2014; Nr. 125. Available online: https://narodne-novine.nn.hr/clanci/sluzbeni/2014_10_125_2382.html (accessed on 5 February 2026).

14. Republic of Croatia. *National Program for Implementation of Strategy of Radioactive Waste, Disused Sources and Spent Nuclear Fuel Management (Program till 2025 with Glance till 2060)*; Republic of Croatia: Zagreb, Croatia, 2018. Available online: https://civilna-zastita.gov.hr/UserDocsImages/dokumenti/Radioloska%20i%20nuklearna%20sigurnost/Nacionalni%20programi/Nacionalni%20program%20provedbe%20Strategije%20zbrinjavanja%20radioaktivnog%20otpada%20iskoristenih%20izvora%20i%20istrosenog%20nuklearnog%20goriva.pdf (accessed on 5 February 2026).
15. Bituh, T.; Petrinec, B.; Skoko, B.; Babić, D.; Rašeta, D. Phosphogypsum and its potential use in Croatia: Challenges and opportunities. *Arch. Ind. Hyg. Toxicol.* **2021**, *72*, 93–100. [CrossRef]
16. Alcordo, I.S.; Rechcigl, J.E. Phosphogypsum in Agriculture: A Review. *Adv. Agron.* **1993**, *49*, 55–118. [CrossRef]
17. Pliaka, M.; Gaidajis, G. Potential uses of phosphogypsum: A review. *J. Environ. Sci. Health. Part A* **2022**, *57*, 746–763. [CrossRef]
18. Murali, G.; Azab, M. Recent research in utilization of phosphogypsum as building materials: Review. *J. Mater. Res. Technol.* **2023**, *25*, 960–987. [CrossRef]
19. Gao, L.; Li, R.; Yang, D.; Bao, L.; Zhang, N. Phosphogypsum improves soil and benefits crop growth: An effective measure for utilizing solid waste resources. *Sci. Rep.* **2025**, *15*, 11827. [CrossRef]
20. Veinović, Ž.; Prlić, I.; Kujundžić, T.; Surić Mihić, M.; Perković, D.; Domitrović, D.; Korman, T.; Mostečak, A.; Uroić, G. Residues Management within the National Program for the Implementation of the Strategy for the Management of Radioactive Waste, Disused Sources and Spent Nuclear Fuel of the Republic of Croatia. *Kem. Ind.* **2020**, *69*, 163−174. [CrossRef]
21. Prlić, I. *Implementation of Radiological Investigative Works in the City of Kaštela at the Location of the Former Jugovinil Factory and Its Surroundings*; Final Report of the Project—Volume I; Institute for Medical Research and Occupational Health & Environmental Protection and Energy Efficiency Fund: Zagreb, Croatia, 2011.
22. Prlić, I. *Radiological Measurements in the City of Kaštela at the Location of the Former Jugovinil Factory and Its Surroundings*; Final Report of the Project—Volume II; Institute for Medical Research and Occupational Health & Environmental Protection and Energy Efficiency Fund: Zagreb, Croatia, 2011.
23. Prlić, I. *Calculation of the Volume of Coal Slag and Ash Located in the City of Kaštela at the Location of the Former Jugovinil Factory and its Surroundings*; Final Report of the Project—Volume III; Institute for Medical Research and Occupational Health & Environmental Protection and Energy Efficiency Fund: Zagreb, Croatia, 2011.
24. Prlić, I. *Research of Documentation Important for the Implementation of Radiological Investigation Works in the City of Kaštela at the Location of the Former Jugovinil Factory and Its Surroundings*; Final Report of the Project—Volume IV; Institute for Medical Research and Occupational Health & Environmental Protection and Energy Efficiency Fund: Zagreb, Croatia, 2011.
25. Socialist Federative Republic of Yugoslavia. *Decision of Republic Secretariat for National Health and Social Protection—Sanitary Inspectorate Concerning the Permanent Disposal of Uranium Ore Tailings in the Grounds of the "Jugovinil" Factory in the Kaštel Gomilica*; Ref.No. UP-I-05-110/1-1974; Socialist Federative Republic of Yugoslavia: Zagreb, Croatia, 1974.
26. Bondžić, D. *Between Ambitions and Illusions—Nuclear Policy of Yugoslavia 1945–1990*; Institut za savremenu istoriju: Belgrade, Serbia, 2016.
27. Skoko, B.; Radić Brkanac, S.; Kuharić, Ž.; Jukić, M.; Štrok, M.; Rovan, L.; Zgorelec, Ž.; Perčin, A.; Prlić, I. Does exposure to weathered coal ash with an enhanced content of uranium-series radionuclides affect flora? Changes in the physiological indicators of five referent plant species. *J. Hazard. Mater.* **2023**, *441*, 129880. [CrossRef]
28. Huang, W.H.; Chen, Z.M.; Chen, T.C.; Yeh, Y.L. Assessing Radiological Risks of Natural Radionuclides on Soil. *Sustainability* **2025**, *17*, 691. [CrossRef]
29. Hernández-Ramírez, D.; Ríos-Martínez, C.; Pinedo-Vega, J.L.; Mireles-García, F.; De la Torre Aguilar, F.; Escareño-Juárez, E. Spatial Distribution and Radiological Risk Assessment of Natural Radionuclides in Soils from Zacatecas, Mexico. *Analytica* **2025**, *6*, 20. [CrossRef]
30. Parizanganeh, A.; Hajisoltani, P.; Zamani, A. Concentration, Distribution and Comparison of Total and Bioavailable Metals in Top Soils and Plants Accumulation in Zanjan Zinc Industrial Town-Iran. *Proc. Environ. Sci.* **2010**, *2*, 167–174. [CrossRef]
31. Nourbakhsh, N.S. Calculation of the Correlation Coefficient of Heavy Metals of Chromium and Cadmium around Qayen Cement Plant. *World J. Environ. Bios.* **2020**, *9*, 40–47.
32. Dragović, S.; Mihailović, N.; Gajić, B. Heavy metals in soils: Distribution, relationship with soil characteristics and radionuclides and multivariate assessment of contamination sources. *Chemosphere* **2008**, *72*, 491–495. [CrossRef]
33. Rafiei, B.; Bakhtiari, N.M.; Hashemi, M.; Khodaei, A.S. Distribution of Heavy Metals around the Dashkasan Au Mine. *Int. J. Environ. Res.* **2010**, *4*, 647–654. [CrossRef]
34. Zhao, Z.; Zhao, Z.; Fu, B.; Wu, D.; Wang, J.; Tang, W. Available Heavy Metal Concentrations and their Influencing Factors in Cropland and Fallows of Different Age in Tropical Area. *Pol. J. Environ. Stud.* **2021**, *30*, 1935–1942. [CrossRef]
35. Hanpattanakit, P.; Taechanitinun, P. Distribution of Heavy Metals and Relationship of Heavy Metals from Land Used in Bangkok, Thailand. *Chem. Eng. Trans.* **2023**, *106*, 577–582. [CrossRef]
36. Louhar, G.; Yaday, R.; Pawar, A.B.; Rekwar, R.K.; Verma, A.K.; Yadav, D.K. Heavy metals distribution and their correlation with physico-chemical properties of different soil series of northwestern India. *Ind. J. Agric. Sci.* **2020**, *90*, 1742–1746. [CrossRef]

37. Rakesh, S.M.S.; Raju, N.S. Correlation of heavy metal contamination with soil properties of industrial areas of Mysore, Karnataka, India by Cluster Analysis. *Int. Res. J. Environ. Sci.* **2013**, *2*, 22–27.
38. Altan, M.; Ayyıldız, Ö.; Malkoc, S.; Yazici, B.; Koparal, S. Heavy Metal Distribution Map in Soil by Using GIS Techniques. *J. Environ. Sci. Eng.* **2011**, *5*, 15–20.
39. Lee, C.S.-L.; Li, X.; Shi, W.-Z.J.; Cheung, S.C.N.; Thornton, I. Metal contamination in urban, suburban, and country park soils of Hong Kong: A study based on GIS and multivariate statistics. *Sci. Total Environ.* **2006**, *356*, 45–61. [CrossRef]
40. Leventeli, Y.; Yalcin, F. Data analysis of heavy metal content in riverwater: Multivariate statistical analysis and inequality expressions. *J. Inequal. Appl.* **2021**, *2021*, 14. [CrossRef]
41. Sohrabizadeh, Z.; Sodaeizadeh, H.; Hakimzadeh, M.A.; Taghizadeh-Mehrjardi, R.; Ghanei Bafghi, M.J. A statistical approach to study the spatial heavy metal distribution in soils in the Kushk Mine, Iran. *Geosci. Data J.* **2023**, *10*, 315–327. [CrossRef]
42. Industrial Applications and Chemistry Section. *Soil Sampling for Environmental Contaminants*; IAEA-TECDOC-1415; International Atomic Energy Agency: Vienna, Austria, 2004.
43. Zečević, M. *Accreditation Certificate for the Institute for Medical Research and Occupational Health, Zagreb, Croatia, According to HRN EN ISO/IEC 17025:2017*; Ref.No.: 383-02/20-30/036; Id.No.: 569-03/2-24-24; Croatian Acreditation Agency: Zagreb, Croatia, 2024.
44. *ISO/IEC 17025:2017*; General Requirements for the Competence of Testing and Calibration Laboratories. International Organization for Standardization: Geneva, Switzerland, 2017.
45. TIBCO Software Inc. *Statistica*, Version 14. Data Analysis Software System. TIBCO Software Inc.: Palo Alto, CA, USA, 2020.
46. Altıkulaç, A.; Turhan, Ş.; Kurnaz, A.; Gören, E.; Duran, C.; Hançerlioğulları, A.; Aysun Uğur, F. Assessment of the Enrichment of Heavy Metals in Coal and Its Combustion Residues. *ACS Omega* **2022**, *7*, 21239–21245. [CrossRef] [PubMed]
47. Popescu, L.G.; Cruceru, M.; Predeanu, G.; Volceanov, E.; Abagiu, A.T.; Bălănescu, M.; Popa, R.; Schiopu, E.C. Analysis of heavy metal content to evaluate leaching characteristics of coal ash wastes. In *Proceedings of the International Multidisciplinary Scientific GeoConference: SGEM, Albena, Bulgaria, 11–15 June 2007*; SGEM: Sofia, Bulgaria, 2013; pp. 33–39.
48. Parzentny, H.R.; Róg, L. Distribution and Mode of Occurrence of Co, Ni, Cu, Zn, As, Ag, Cd, Sb, Pb in the Feed Coal, Fly Ash, Slag, in the Topsoil and in the Roots of Trees and Undergrowth Downwind of Three Power Stations in Poland. *Minerals* **2021**, *11*, 133. [CrossRef]
49. Fernández-Turiel, J.L.; de Carvalho, W.; Cabañas, M.; López-Soler, A. Mobility of heavy metals from coal fly ash. *Environ. Geol.* **1994**, *23*, 264–270. [CrossRef]
50. Čustović, H.; Žurovec, O. Environmental Impact of Coal Ash Deposition. In Proceedings of the 10th Alps-Adria Scientific Workshop, Opatija, Croatia, 14–19 March 2011.
51. Santos, A.C.; Cruz, C.; Font, E.; French, D.; Guedes, A.; Moreira, K.; Sant'Ovaia, H.; Vieira, B.J.C.; Waerenborgh, J.C.; Valentim, B. Physicochemical Properties of Fe-Bearing Phases from Commercial Colombian Coal Ash. *Minerals* **2023**, *13*, 1055. [CrossRef]
52. Biswas, A.; Hendry, M.J.; Essilfie-Dughan, J.; Day, S.; Villeneuve, S.A.; Barbour, S.L. Geochemistry of zinc and cadmium in coal waste rock, Elk Valley, British Columbia, Canada. *Appl. Geochem.* **2022**, *136*, 105148. [CrossRef]
53. Pongrac, P.; Troskot-Čorbić, T.; Durn, G. Impact of coal depository and slag disposal from the Plomin thermal power plant on soil composition: Insights from geochemical, mineralogical, and organic petrological analyses, Istria, Croatia. *Geol. Croat.* **2024**, *77*, 179–191. [CrossRef]
54. López Antón, M.A.; Spears, D.A.; Díaz Somoano, M.; Martínez Tarazona, M.R. Thallium in coal: Analysis and environmental implications. *Fuel* **2013**, *105*, 13–18. [CrossRef]
55. Karbowska, B. Presence of thallium in the environment: Sources of contaminations, distribution and monitoring methods. *Environ. Monit. Assess.* **2016**, *188*, 640. [CrossRef]
56. Esri. *ArcGIS Pro*, Version 3.6. Geographic Information System Software for Spatial Analysis and Geostatistics. Esri: Redlands, CA, USA, 2024.
57. Amoroso, P.P.; Aguilar, F.J.; Parente, C.; Aguilar, M.A. Statistical Assessment of Some Interpolation Methods for Building Grid Format Digital Bathymetric Models. *Remote Sens.* **2023**, *15*, 2072. [CrossRef]
58. Piazza, A.D.; Conti, F.L.; Viola, F.; Eccel, E.; Noto, L.V. Comparative Analysis of Spatial Interpolation Methods in the Mediterranean Area: Application to Temperature in Sicily. *Water* **2015**, *7*, 1866–1888. [CrossRef]
59. Bezyk, Y.; Sówka, I.; Górka, M.; Blachowski, J. GIS-Based Approach to Spatio-Temporal Interpolation of Atmospheric $CO_2$ Concentrations in Limited Monitoring Dataset. *Atmosphere* **2021**, *12*, 384. [CrossRef]
60. Caloiero, T.; Pellicone, G.; Modica, G.; Guagliardi, I. Comparative Analysis of Different Spatial Interpolation Methods Applied to Monthly Rainfall as Support for Landscape Management. *Appl. Sci.* **2021**, *11*, 9566. [CrossRef]
61. Igaz, D.; Šinka, K.; Varga, P.; Vrbičanová, G.; Aydın, E.; Tárník, A. The Evaluation of the Accuracy of Interpolation Methods in Crafting Maps of Physical and Hydro-Physical Soil Properties. *Water* **2021**, *13*, 212. [CrossRef]
62. Gribov, A.; Krivoruchko, K. Empirical Bayesian kriging implementation and usage. *Sci. Total Environ.* **2020**, *722*, 137290. [CrossRef] [PubMed]
63. Krivoruchko, K.; Gribov, A. Evaluation of empirical Bayesian kriging. *Spat. Stat.* **2019**, *32*, 100368. [CrossRef]

64. Zaresefat, M.; Derakhshani, R.; Griffioen, J. Empirical Bayesian Kriging, a Robust Method for Spatial Data Interpolation of a Large Groundwater Quality Dataset from the Western Netherlands. *Water* **2024**, *16*, 2581. [CrossRef]
65. Mrdakovic Popic, J.; Vanhoudt, N.; Venoso, G.; Leonardi, F.; Haanes, H.; Dvorzhak, A.; Nuccetelli, C.; Trevisi, R.; Ugolini, R.; Trotti, F.; et al. A Systematic Review of Naturally Occurring Radioactive Materials (NORM) in Energy Production Sectors: Exposure, Effective Doses and Regulatory Challenges. 2025. Available online: https://ssrn.com/abstract=5270528 (accessed on 1 December 2025).
66. Sumary, D.P.; Raymond, J.; Chacha, M.; Banzi, F.P. Assessment of radiation exposure from naturally occurring radioactive materials in Bahi district, Tanzania, using RESRAD-BIOTA modeling. *Bull. Natl. Res. Cent.* **2025**, *49*, 88. [CrossRef]
67. Maina, P.K. The Exposure of Terrestrial Biota to Naturally Occurring Radiation and Stable Elements: Case Orrefjell, a Risk Assessment. Master's Thesis, Norwegian University of Life Sciences, Ås, Norway, May 2018. Available online: https://static02.nmbu.no/mina/studier/moppgaver/2018-Maina.pdf (accessed on 14 November 2025).
68. MacIntosh, A.; Koppel, D.; Johansen, M.; Beresford, N.; Copplestone, D.; Penrose, B.; Cresswell, T. Radiological risk assessment to marine biota from exposure to NORM from a decommissioned offshore oil and gas pipeline. *J. Environ. Radioact.* **2022**, *251–252*, 106979. [CrossRef]
69. Ministry of Agriculture, Forestry and Fishery. *Ordinance on Protection of Agricultural Land from Pollution*; Official Gazette: Zagreb, Croatia, 2019; Nr. 71. Available online: https://narodne-novine.nn.hr/clanci/sluzbeni/2019_07_71_1507.html (accessed on 5 February 2026).
70. State Office for Nuclear Safety. *Regulations on Monitoring the State of Radioactivity in the Environment*; Official Gazette: Zagreb, Croatia, 2018; Nr. 40. Available online: https://narodne-novine.nn.hr/clanci/sluzbeni/2018_05_40_776.html (accessed on 5 February 2026).
71. Isplate.info. Monthly Pool of Hours for the Year 2025. Available online: https://isplate.info/fond-sati-2025 (accessed on 5 February 2026).
72. IAEA. *The Environmental Behaviour of Radium: Revised Edition*; Technical Report; IAEA Technical Report Series No. 476; IAEA: Vienna, Austria, 2014. Available online: https://www-pub.iaea.org/MTCD/Publications/PDF/trs476web-45482131.pdf (accessed on 7 December 2025).
73. Omeje, M.; Olusegun, A.O.; Joel, E.S.; Ehi-Eromosele, C.O.; PraiseGod, E.C.; Usikalu, M.R.; Akinwumi Sayo, A.; Zaidi, E.; Saeed, M.A. Natural radioactivity concentrations of $^{226}$Ra, $^{232}$Th, and $^{40}$K in commercial building materials and their lifetime cancer risk assessment in dwellers. *Hum. Ecol. Risk Assess. Int. J.* **2018**, *24*, 2036–2053. [CrossRef]
74. Mehra, R. Use of Gamma Ray Spectroscopy Measurements for Assessment of the Average Effective Dose from the Analysis of $^{226}$Ra, $^{232}$Th, and $^{40}$K in Soil Samples. *Indoor Built Environ.* **2009**, *18*, 270–275. [CrossRef]
75. Dutra Garcêz, R.W.; Lopes, J.M.; Frota Lima, M.A.; da Silva, A.X. Determination of Ra-226, Ra-228 and K-40 specific activities in samples of mineral fertilizers marketed in the city of Rio de Janeiro, Brazil. *Appl. Radiat. Isot.* **2018**, *141*, 199–202. [CrossRef]
76. IAEA. *IAEA Safety Standards, General Safety Requirements GSR Part 3. Radiation Protection and Safety of Radiation Sources: International Basic Safety Standards*; IAEA: Vienna, Austria, 2014. Available online: https://www-pub.iaea.org/MTCD/Publications/PDF/Pub1578_web-57265295.pdf (accessed on 7 December 2025).
77. Liu, L.; Li, W.; Song, W.; Guo, M. Remediation techniques for heavy metal-contaminated soils: Principles and applicability. *Sci. Total Environ.* **2018**, *633*, 206–219. [CrossRef]
78. Croatian Meteorological and Hydrological Service. Available online: https://meteo.hr/index_en.php (accessed on 5 February 2026).